2017-03

Fabrication of high energy density tin/carbon anode using reduction expansion synthesis and aerosol through plasma techniques

Lim, Tongli

Monterey, California: Naval Postgraduate School

NAVAL POSTGRADUATE SCHOOL

MONTEREY, CALIFORNIA

THESIS

FABRICATION OF HIGH ENERGY DENSITY TIN/ CARBON ANODE USING REDUCTION EXPANSION SYNTHESIS AND AEROSOL THROUGH PLASMA TECHNIQUES

by

Tongli Lim

March 2017

Thesis Advisor: Jonathan Phillips
Co-Advisor: Claudia Luhrs

THIS PAGE INTENTIONALLY LEFT BLANK

REPORT DOCUMENTATION PAGE			*Form Approved OMB No. 0704–0188*

1. AGENCY USE ONLY *(Leave blank)*	**2. REPORT DATE** March 2017	**3. REPORT TYPE AND DATES COVERED** Master's thesis

4. TITLE AND SUBTITLE FABRICATION OF HIGH ENERGY DENSITY TIN/CARBON ANODE USING REDUCTION EXPANSION SYNTHESIS AND AEROSOL THROUGH PLASMA TECHNIQUES	**5. FUNDING NUMBERS**
6. AUTHOR(S) Tongli Lim	
7. PERFORMING ORGANIZATION NAME(S) AND ADDRESS(ES) Naval Postgraduate School Monterey, CA 93943-5000	**8. PERFORMING ORGANIZATION REPORT NUMBER**
9. SPONSORING /MONITORING AGENCY NAME(S) AND ADDRESS(ES) N/A	**10. SPONSORING / MONITORING AGENCY REPORT NUMBER**

11. SUPPLEMENTARY NOTES The views expressed in this thesis are those of the author and do not reflect the official policy or position of the Department of Defense or the U.S. Government. IRB number ____N/A____.

12a. DISTRIBUTION / AVAILABILITY STATEMENT Approved for public release. Distribution is unlimited.	**12b. DISTRIBUTION CODE**

13. ABSTRACT (maximum 200 words)

The aim of this study was to fabricate tin/carbon (Sn/C) battery anodes using a novel approach, reduction expansion synthesis (RES), and test their performance as electrodes in lithium or sodium batteries. A second preparation route, the Aerosol-Through-Plasma (ATP) method, was also employed for comparison. The specimens generated were characterized, before and after cycling, using techniques such as X-ray diffraction, scanning, and transmission electron microscopy. The RES technique was successful in creating remarkably small (ca. <5 nm) nano-scale particles of tin dispersed on the carbon support. The use of the electrodes as part of coin cell batteries resulted in capacitance values of 320 mAh/g and 110 mAh/g for lithium-ion and sodium-ion batteries, respectively. Nano-sized Sn particles were found before and after cycling. It is believed that bonds between metal atoms and dangling carbon produced via the reduction of the carbon surface during RES were responsible for the materials' ability to withstand stresses during lithiation, avoid volumetric expansion, and prevent disintegration after hundreds of cycles. When tin loading in Sn/C was increased from 10% to 20%, an increase of capacitance from 280 mAh/g to 320mAh/g was observed; thus, increased tin loading is recommended for future studies. Tin/carbon produced using ATP presented morphology consistent with stable electrodes, although battery testing was not completed because of the difficulty of producing the material in sufficient quantity.

14. SUBJECT TERMS electrodes, batteries, nanoparticles, RES, ATP, Sn/C anodes			**15. NUMBER OF PAGES** 99
			16. PRICE CODE
17. SECURITY CLASSIFICATION OF REPORT Unclassified	**18. SECURITY CLASSIFICATION OF THIS PAGE** Unclassified	**19. SECURITY CLASSIFICATION OF ABSTRACT** Unclassified	**20. LIMITATION OF ABSTRACT** UU

NSN 7540–01-280-5500 Standard Form 298 (Rev. 2–89) Prescribed by ANSI Std. 239–18

THIS PAGE INTENTIONALLY LEFT BLANK

Approved for public release. Distribution is unlimited.

FABRICATION OF HIGH ENERGY DENSITY TIN/CARBON ANODE USING REDUCTION EXPANSION SYNTHESIS AND AEROSOL THROUGH PLASMA TECHNIQUES

Tongli Lim
Military Expert 5, Republic of Singapore Navy
B.Eng., National University of Singapore, 2006

Submitted in partial fulfillment of the
requirements for the degree of

MASTER OF SCIENCE IN MECHANICAL ENGINEERING

from the

NAVAL POSTGRADUATE SCHOOL
March 2017

Approved by: Jonathan Phillips
Thesis Advisor

Claudia Luhrs
Co-Advisor

Garth V. Hobson
Chair, Department of Mechanical and Aerospace Engineering

THIS PAGE INTENTIONALLY LEFT BLANK

ABSTRACT

The aim of this study was to fabricate tin/carbon (Sn/C) battery anodes using a novel approach, reduction expansion synthesis (RES), and test their performance as electrodes in lithium or sodium batteries. A second preparation route, the Aerosol-Through-Plasma (ATP) method, was also employed for comparison. The specimens generated were characterized, before and after cycling, using techniques such as X-ray diffraction, scanning, and transmission electron microscopy. The RES technique was successful in creating remarkably small (ca. <5 nm) nano-scale particles of tin dispersed on the carbon support. The use of the electrodes as part of coin cell batteries resulted in capacitance values of 320 mAh/g and 110 mAh/g for lithium-ion and sodium-ion batteries, respectively. Nano-sized Sn particles were found before and after cycling. It is believed that bonds between metal atoms and dangling carbon produced via the reduction of the carbon surface during RES were responsible for the materials' ability to withstand stresses during lithiation, avoid volumetric expansion, and prevent disintegration after hundreds of cycles. When tin loading in Sn/C was increased from 10% to 20%, an increase of capacitance from 280 mAh/g to 320mAh/g was observed; thus, increased tin loading is recommended for future studies. Tin/carbon produced using ATP presented morphology consistent with stable electrodes, although battery testing was not completed because of the difficulty of producing the material in sufficient quantity.

THIS PAGE INTENTIONALLY LEFT BLANK

TABLE OF CONTENTS

LIST OF FIGURES

THIS PAGE INTENTIONALLY LEFT BLANK

LIST OF TABLES

THIS PAGE INTENTIONALLY LEFT BLANK

LIST OF ACRONYMS AND ABBREVIATIONS

ATP	Aerosol-Through-Plasma
EDS	Energy Dispersive X-Ray Spectroscopy
FEC	Fluoroethylene Carbonate
FWHM	Full Width Half Maximum
RES	Reduction Expansion Synthesis
SEM	Scanning Electron Microscopy
TEM	Transmission Electron Microscopy
USN	United States Navy
XRD	X-Ray Diffraction

THIS PAGE INTENTIONALLY LEFT BLANK

EXECUTIVE SUMMARY

This study was motivated by the need for improved batteries, an enabling technology for the proposed all-electric ship Navy. In particular, the work conducted was designed to study a narrow aspect of improved battery performance: the use of tin/carbon (Sn/C) electrodes in both lithium-ion and sodium-ion batteries. In theory, Sn/C electrodes can improve the capacity (total current delivered) by a factor of 2.5 relative to standard carbon electrode batteries. Despite numerous studies, a robust battery based on Sn electrodes has never been satisfactorily demonstrated. The impact of Sn/C electrodes in sodium-ion batteries is not theoretically as significant as that of Sn/C, but has the strategic advantage of potentially reducing the dependence of battery technology on lithium, which is not found in sufficient quantity in the United States.

The unique aspect of this study relative to other studies of Sn/C electrodes is the use of a novel approach known as Reduction Expansion Synthesis (RES) to create Sn/C electrodes that have high-energy densities when placed in a lithium (Li)- and sodium (Na)-ion battery. The products were tested as coin cell lithium/sodium-ion batteries and characterized before and after hundreds of cycles, using techniques such as X-ray diffraction and electron microscopy. Results showed that the RES technique was successful in creating remarkably small (ca. <5 nm) and stable nano-scale particles of Sn produced on the carbon with capacitance values of 320 mAh/g and 110 mAh/g for Li-ion and Na-ion batteries, respectively.

The results also prove that the fundamental materials hypothesis tested in this thesis is true. Dangling carbon bonds produced on the carbon surface during the RES synthesis bond with Sn atoms produces a strong and direct carbon-metal bond that is able to withstand the volumetric expansion of tin that occurs during cyclic loading with either Li or Na (~450%). In contrast, Sn/C electrodes using more traditional synthesis techniques are not stable, and tend to disintegrate due to volumetric expansion during lithiation. This results in a rapid loss of battery capacitance.

It is postulated that the stable capacitance observed for Sn/C anodes formed using RES relative to more traditional synthesis techniques results from the formation of uniquely strong bonds between carbon and Sn when the RES method is employed. That is, this study suggests that Sn/C produced using the RES technique creates a very strong tin/carbon bond that stabilizes Sn particles, preventing sintering and Sn particle growth during battery cycling, with both lithium and sodium ions. However, further studies are required to prove the capacitance values when these materials are used in a battery.

In summary, Sn/C samples produced by RES have been tested as anodes for Na/ Li-ion batteries, and these initial tests were successful in demonstrating unique stability over many cycles. The method of anode production is commercially viable as it is a simple method that can be easily scalable. This initial finding in producing high-energy density tin/carbon anodes could pave the way for future production of sodium-ion batteries. This would allow the U.S. Navy to be less dependent on lithium. Sodium, as compared to lithium, is less expensive and more readily available. This would be an important prospect especially as the U.S. Navy enters the age of electric warships, utilizing energy-intensive weapons such as free electron lasers and rail guns that would require better energy storage mediums in the future.

ACKNOWLEDGMENTS

I would like to thank my advisor, Professor Jonathan Phillips, for sharing his wealth of knowledge in the field of materials engineering, particularly for the RES method and the production of a metallic catalyst on an activated carbon support. It was his vision that started this study, and his constant drive made this study a success. I would also like to thank my co-advisor, Professor Claudia Luhrs, for her patience and guidance throughout the study. In particular, I would like to thank Professor Luhrs for providing foundational knowledge in nanomaterials and introducing me to the ATP method.

I would like to take the opportunity to thank Professor Hugo Zea, who was always available to provide insights to the study. In particular, he provided me with a background to the porosity of carbons that prompted the use of a different carbon support, leading to the success of the study. I would also like to thank Professor Sarath Menon for his assistance with the analysis of samples using the TEM, as well as teaching me the safe use of XRD and SEM. Special thanks also go out to Ryan Adams and Professor Vilas Pol from the Chemical Engineering department of Purdue University in the testing of samples in a battery cell.

To my superiors, SLTC Lim Khia Teck, LTC (Ret) Lee Wai Lum, and LTC Neo Kim Hang of the Republic of Singapore Navy (RSN), thank you for having the confidence in me and allowing me to pursue this master's degree. Special thanks go out to my buddies from RSS Vigour, MSTF and OCS for encouraging me in this pursuit.

To my parents, Dr. Lim Wei How and Ms. Ng Ah Moi, thank you for your unwavering support throughout the span of the thesis and the pursuit of my degree at the Naval Postgraduate School. Your love and constant calls from Singapore have been instrumental in supporting me in this endeavor. To my beloved wife, Ms. Yap Karen, thank you for always being there and taking good care of me throughout our time in Monterey. It was your patience and love that supported me through the many hours spent at the laboratory in creating and analyzing the materials.

I thank the Lord Jesus Christ for His blessings in completing this master's degree.

THIS PAGE INTENTIONALLY LEFT BLANK

I. INTRODUCTION

With the development of weapons such as the rail gun [1] and free electron laser [2], there is now a greater emphasis by the United States Navy (USN) to develop platforms able to accommodate these systems. Specifically, plans call for all electric ships in which everything from drives to weapons will be run using electric energy. The Zumwalt-class destroyer is one such platform that is expected to commence testing of the rail gun by 2018 [3]. This transformation requires developing cheaper, highly reliable, always available, battery forms with higher energy densities as compared to the current lithium-ion batteries.

Sodium-ion batteries are an attractive alternative to lithium because unlike lithium, sodium is found virtually everywhere. According to the U.S. Geological Survey of Mineral Commodities in 2016, lithium resources in the United States is approximately 6.7 million tons, with approximately 34 million tons residing in other countries [4]. As solar energy products and electric cars begin to compete for the same lithium reserve, this finite resource will be depleted at an increasing pace. On the other hand, if sodium-ion batteries are developed, there would be no need to protect such a strategic reserve. However, free energy calculation for sodium shows that the reaction chemistry powering electrons in a sodium battery produces less energy than the equivalent reaction in a lithium battery [5]. Tin/sodium chemistry appears appropriate for sodium to compete with lithium. Although tin is a viable material for low-density, high-energy reaction chemistry in sodium batteries, it expands up to 300% during cyclic loading, leading to mechanical damage and short battery life [6]. Hence, this research project was designed to explore means to stabilize a tin/alkali battery by creating stronger bonds between tin and carbon, which will mechanically stabilize the tin (Sn) particles.

In addition to tin/sodium chemistry, lithium/sodium (Li/Na) chemistry also shows promising values in terms of the high final stoichiometry of Li/Sn. With $Li_{22}Sn_5$, the resulting high lithium packing density (75.47 mol L^{-1}) is nearly as high as that of pure lithium metal, which has a packing density of 76.36 mol L^{-1} [7]. This packing density yields a theoretical ~990 mAh/g Sn [8]. This is far better than that of the ultimate

graphite electrode, ~370 mAh/g C, because in the graphite system the final stoichiometry is believed to be 1Li/6C [9]. The intent is to mechanically stabilize tin particles during sodium uptake, thus increasing battery life. Specifically, novel synthesis techniques such as the Reduction Expansion Synthesis (RES) and Aerosol Through Plasma (ATP) techniques are used.

A. INCREASED ELECTRICAL STORAGE NEEDS IN THE USN

The rail gun (Figure 1) is currently pursued as a weapon of choice by the USN because of its speed and precision. The rail gun has been reported to fire projectiles at speeds of 5,700 miles per hour [10] and is more precise than any weaponry in the current arsenal of the USN. Due to these factors, it has been touted as a "game changer" [11] because it forces an unfamiliar form of weaponry unto its adversaries. Current discussions include fielding the rail gun on the third Zumwalt-class destroyer [12].

Figure 1. Rail Gun. Source: [11].

Although the free electron laser (Figure 2) has high electric energy and power requirements, it can provide not only a form of defense against missiles, it is also a

scalable weapon, providing varying lethality options to the USN [13]. In addition, the cost of each shot of lasers is inexpensive and relatively simple to operate, with only one sailor required to fire each shot. A prototype is currently being tested aboard the USS *Ponce* in the Persian Gulf and has already yielded positive results in disabling vessels in its area of operation [14].

Figure 2. Laser Weapon System on USS *Ponce*. Source: [11].

In order to operationalize these weapons, an all-electric ship is required. The Zumwalt-Class destroyer (Figure 3) will be equipped with the Integrated Power System that allows the utilization of energy from prime movers as well as a network of electrical distribution to direct this energy to the weapons [15], [16]. As a result of these power requirements, various methods of battery charging are being developed [17]. Of particular interest in this work is the development of lithium-sodium/carbon (Li-Sn/C)

batteries as an alternative for lithium/carbon (Li/C), and potentially the development of sodium-tin/carbon (Na-Sn/C) batteries.

Figure 3. Zumwalt-Class Destroyer. Source: [15].

The Zumwalt-Class Destroyer is the USN's first all-electric ship, which is designed to incorporate future weaponry such as the free electron laser.

B. TIN/CARBON AS AN ALTERNATIVE FOR SODIUM-ION BATTERIES

Although Li/C (also known as lithium-ion) batteries have been established as a battery of choice, factors such as availability and cost have increased the need to find an alternative material for batteries. Of particular concern to the military is the availability of the materials on which it relies, and the naturally occurring sources of lithium are likely insufficient to meet the needs of the military in the future. In this regard, sodium is a viable alternative to lithium. It is cheaper, more widely available, and most importantly, is chemically similar to lithium. However, free energy calculations show that sodium's

energy density will always be lower than that of lithium [18]. Therefore, for sodium-ion batteries to compete with lithium-ion batteries, a higher energy density anode is required. Tin/carbon anodes are an intriguing alternative to simple and standard carbon anodes because the theoretical capacity of 846mAh/g [19] is nearly three times greater than that of carbon electrodes. Nevertheless, tin-based batteries have never functioned due to volumetric expansions of up to 300%, which lead to mechanical crumbling and concomitant rapid battery aging [20].

Two methods have been studied to mitigate the effects of crumbling during lithiation. The first method attempts to encapsulate Sn within conductive structures with void spaces that permit expansion without concomitant breakage. This method yields high, ~600 mAh/g, and sometimes very high, ~1500 mAh/g [21–24], initial capacity but little stability, as in all measured cases the capacity declines with each cycle. In this thesis, the second and novel tin anode synthesis method designed to prevent crumbling of tin is studied.

The basis of this proposed alternative synthesis approach can be traced back decades to early studies of the surface chemistry of activated carbon. Walker et al. [25] started work on the study of activated carbon. Their work showed that there is a large change in adsorption properties when carbon is heated to 1000 degrees Celsius. Phillips et al. [26] later showed that there is a difference in carbon surface structure and adsorption properties based not simply on temperature but also gas phase present during heating. Specifically, heating in nitrogen gas creates a far different surface than heating in hydrogen gas. Heating in nitrogen creates a surface full of unsaturated carbon atoms, or surface radicals. Heating in hydrogen, in contrast, leaves a surface free of active sites. Little or no gas adsorption takes place and the surface is hydrophobic. Figure 4 shows the production of dangling carbon bonds through the adsorption and removal of oxygen on the surface of the carbon. Many of the advancements in understanding the surface chemistry of activated carbon by Phillips et al. [27] resulted from the development and use of microcalorimetry [28]. An example is found in Figure 5. The treatment with nitrogen leaves unsaturated carbon atoms, which are very active for subsequent adsorption of oxygen. In particular, it was found that activated carbon with dangling

bonds can be produced by heating carbon in oxygen and removing the oxygen group under nitrogen flow.

Figure 4. Adsorption and Removal of Oxygen to Produce Dangling Bonds. Source: [26].

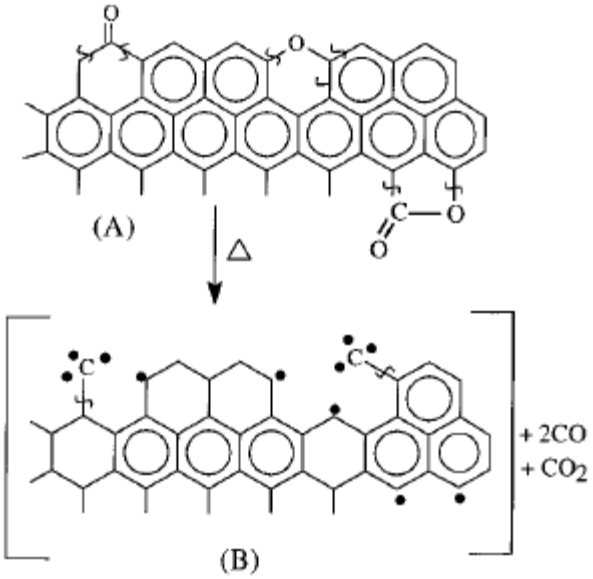

Surface chemistry of carbon. A: Activation of carbon which produces oxides on the surface of the carbon B: Heating of activated carbon produces dangling carbon bonds that are ready for metallic bonding

Studies by Skokova et al. also showed that spillover occurs where oxygen is not only adsorbed on the edge sites of carbon crystallites, but also at the basal plane. This increases the overall amount of oxygen that resides on the surface of the carbon at higher temperatures [29]. Studies done by Phillips et al. revealed that with the use of calorimetry, surface chemistry of a material can be obtained. This is important because the surface chemistry of a material determines processes such as adsorption and the stability of metal particles, which are employed for heterogeneous catalysis and battery electrodes, under application conditions. It was found that when carbon was treated in nitrogen, both lower energy sites and dangling carbon sites were produced as compared to treatment in hydrogen, where only lower energy sites were produced on the surface.

Figure 5. Results of Oxygen Microcalorimetric Studies at 150 Degrees Celsius for Surface-Treated Activated Carbons. Source: [28].

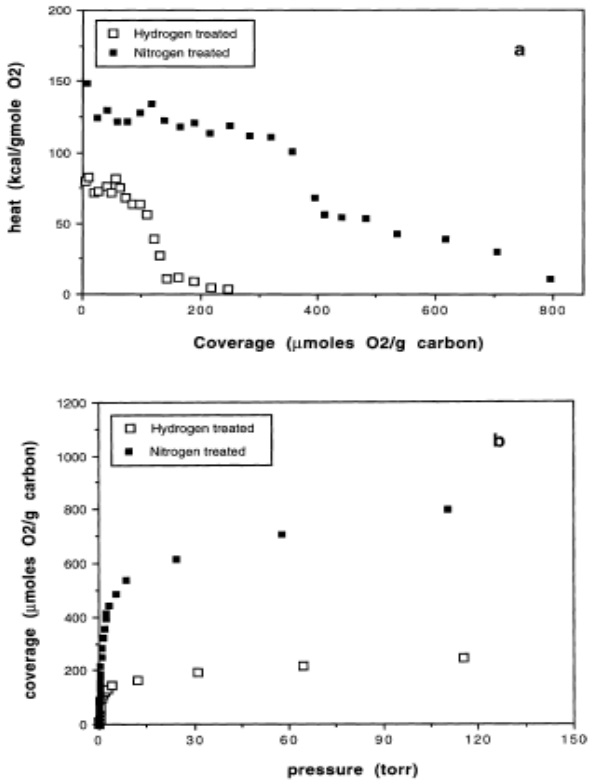

Results of microcalorimetric studies. The amount of oxygen and the strength of the oxygen bonding are both a function of the gas present during heating. Indeed, heating in nitrogen increases both the amount and strength of oxygen bonding. a. Differential Heats as a function of surface coverage showing the production of both lower energy sites and dangling carbon sites. b. Adsorption Isotherms showing carbon activation when heated in nitrogen

Further, iron (Fe) was found to be able to adhere to the dangling carbon bonds, suggesting that metals can also form these unique and strong bonds [30] by attaching to energetic and edge sites produced by nitrogen [31]. Hence, it is postulated that if tin particles are attached to the dangling carbon bonds, a unique bond could be created that avoids sintering and increases cyclability.

In summary, fundamental studies of activated carbon suggested a simple synthesis capable of creating direct chemical links between the carbon substrate and the adsorbed atoms. That is to say, carbon is first heated in an inert atmosphere (e.g., N_2) in excess of 800 degrees Celsius. Subsequently, the desired species is added without exposure to air

and these species will be directly and strongly bonded to carbon atoms in the surface. These bonds will be strong enough to prevent the movement and sintering of atoms, particularly metal atoms bonded to the carbon substrate.

In contrast, if this high temperature and inert gas treatment is not done, bonding of atoms on the surface will occur through oxygen groups that are in turn directly bonded to the carbon. Metal atoms bonded to carbon via oxygen linkages are known to move easily, leading to rapid sintering. The synthesis techniques explored in this thesis were designed to allow direct carbon-metal bonding rather than carbon-oxygen-metal bonding. The intent was to prevent sintering of metal, specifically tin, during battery operation.

C. ADVANCED TECHNIQUES OF RES AND ATP

To achieve the fabrication of a tin/carbon anode with very high tin dispersion and high mechanical stability over many cycles, a new synthesis approach is required. For this thesis, two methods were explored: RES and ATP. RES is a method invented by Luhrs and Phillips, where the precursor utilizes a decomposing solid, generally urea, as a reductive agent [32]. It has been found that the process is capable of producing metals by reducing oxides and hydroxides via the release of reducing radical species that are produced as urea and other solid reducing agents thermally decompose. RES has already been employed to make graphene [32], supported metal catalysts [33], small iron and nickel particles [34], alloys of the same [35], [36] and chromium (Cr) metal coatings on iron. Using a precursor mix of water, urea, tin (II) chloride, and activated carbon, the reduction process removes the oxygen groups on the activated carbon surface via reducing groups produced, allowing tin produced by the thermal decomposition of tin (II) chloride to strongly and directly bond to carbon atoms in the surface. Therefore, tin is strongly attached to the dangling bonds after the removal of oxygen groups.

ATP, on the other hand, is another method of producing the supported metal catalyst. Invented by Phillips et al., ATP is a process in which an aerosol composed of metal powder and support is carried by an aerosol and passed through microwave generated plasma. Aluminum, titania, and alumina nanoparticles have been produced in

such a manner. Hence it is also postulated that the same unique bonds can be produced using Sn particles and carbon.

In the following chapters, the experimental methods, results, discussion, conclusion, and future recommendations are described in detail. Highlights from the ensuing chapters include

- Experimental Methods. Characterization techniques used in the study, such as X-ray diffraction (XRD), Scanning Electron Microscopy (SEM), Energy Dispersive X-ray Spectroscopy (EDS), and Transmission Electron Microscopy (TEM) are described. In addition, the fabrication of Sn/C electrodes using RES and ATP is described in detail. Particularly for the RES technique, emphasis was placed in activating the carbon support, increasing the proportion of Sn particles, and decreasing the size of Sn particles (Figure 6).

Figure 6. Overview of Sn/C Synthesis.

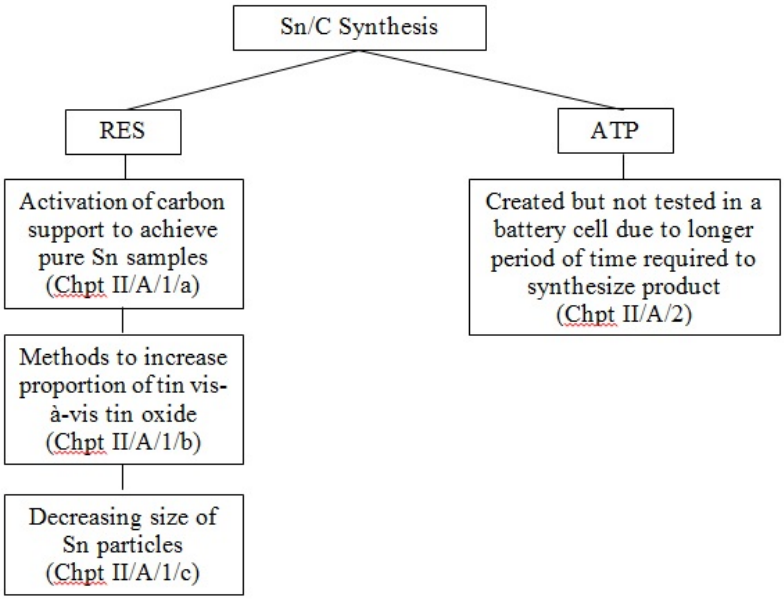

Overview of Sn/C Synthesis. Approaches taken during the study to improve the final Sn/C produced by RES. ATP Sn/C were created but were not tested in a battery as the longer period of time for production did not prove to be an economically viable option.

- Results. Results showed that the steps taken in creating the Sn/C electrodes were successful. In particular, XRD results showed the presence of Sn after cycling while SEM and TEM results showed remarkably small (<5nm) tin particles found before and after cycling,

demonstrating the unusually stable nature of Sn/C created using RES. In addition, Sn/C cycled in a Li-ion and Na-ion battery showed capacity values of 320 mAh/g and 110 mAh/g, respectively. The study also included an increase of tin loading from 10% to 20%, which resulted in an 18% increase in capacity from 280 mAh/g to 320 mAh/g. These results show that the RES technique is successful and has much promise for future development of Na-ion batteries.

- Discussion. The study also demonstrates that with an understanding of the surface chemistry of carbons, the researcher can use activated carbons together with the RES technique to successfully create uniquely strong Sn/C bonds that are remarkably stable and prevent particle growth during cycling. In particular, the RES technique concurrently generates free radicals on the surface of the carbon via thermal decomposition of urea and removes surface oxygen atoms by reducing those radicals to create unsaturated surface sites. The bonding of Sn to these sites has resulted in the strong Sn/C bonds created through RES.

The penultimate chapter of this thesis presents significant results from the studies while the last chapter focuses on the recommendations for future approaches.

II. EXPERIMENTAL METHODS

This chapter consists of two sections that describe the synthesis and characterization of the samples. In the first section, the two methods used for the synthesis of the samples, namely Reduction Expansion Synthesis (RES) and Aerosol Through Plasma (ATP) techniques, are described. Both processes are hypothesized to produce small Sn particles with strong linkage to the carbon support. However, RES would be a better commercial method, given that it utilizes a simpler setup with the option to scale up the process easily. In the second section, characterization techniques such as X-Ray Diffraction (XRD), Scanning Electron Microscopy (SEM), Transmission Electron Microscopy (TEM), and Energy Dispersive X-Ray Spectroscopy (EDS) are discussed.

A. SYNTHESIS

The synthesis of Sn/C anode via the Reduction Expansion Synthesis (RES) and Aerosol Through Plasma (ATP) will be discussed in this section.

1. Reduction Expansion Synthesis

The RES technique is a method invented by Luhrs and Phillips, where a reductive-expansion agent, such as urea, produces reducing gases when heated to high temperatures. Gases released by thermal decomposition are believed to include carbon monoxide (CO), and NHx species that reduce the targeted material to form the desired particles in its zero valence form. The entire process takes place in a furnace under an inert atmosphere and the sample is heated to a temperature higher than the decomposition temperature of urea (typically above 600 degrees Celsius).

The series of experiments began with precursors of tin (II) acetate, urea, carbon, and water, mixed in the ratio of 1: 1: 2.5: 20. Water, as part of the precursor, helps to dissolve the Sn compound and distribute the Sn precursors and urea into the carbon support. The idea is to distribute the precursor thoroughly, such that upon decomposition by heating, Sn precursor density is the same on all carbon surfaces. The intention is to produce small Sn particles homogeneously after reduction. However, it was found that tin

(II) acetate has a poor solubility in water, which prevents the distribution of Sn into the carbon support. Hence, tin (II) chloride was subsequently used as it readily dissolves in water. Subsequently, an aqueous solution of tin (II) chloride and urea can readily distribute evenly on the surface of a hydrophilic carbon powder.

a. Activating the Carbon Support

Prior to mixing the precursors together, the carbon is preheated in air to a temperature of 600 degrees Celsius for ten minutes (Figure 7). This process allows oxygen to be attached to the surface of the carbon. It is these surface oxygens that create the hydrophilic condition required to allow dispersion of the precursor via surface wetting. This oxygen will subsequently be reduced during the reduction-expansion phase. Some of the reducing radicals released during thermal decomposition of urea will remove the surface oxygen, creating dangling carbon bonds that react strongly with Sn precursor. This creates a unique and strong bond between metal and carbon support as previously observed for Fe bonding to a carbon containing dangling bonds. Net result: the tin particles adhere strongly to the carbon support and resist sintering. In contrast, traditional incipient wetness production produces Sn that is poorly bonded to carbon, generally via oxygen-atom linkages, which rapidly sinters to produce micron scale particles.

Figure 7. Carbon Heated in Air to 600 Degrees Celsius.

Activation of carbon. Activation of carbon by heating in a furnace exposed to air. Oxygen groups attach to the surface of carbon activating it for the RES process. Fans facilitated the movement of air during activation.

b. Steps in Creating Sn/C Sample via RES

To create a product of approximately 1gram, 0.4g of tin (II) chloride, 0.4g of urea, 1g of carbon, and 8g of water are mixed and hand ground using a mortar and pestle set to produce a paste (Figure 8). Depending on the porosity of the carbon support, the mortar and pestle set helps to mechanically distribute the Sn precursor and urea throughout the carbon support. Thereafter, the paste is placed into the furnace via an alumina boat (Figure 9).

Figure 8. Precursor of Tin (II) Chloride, Urea, and Water to Form a Solution.

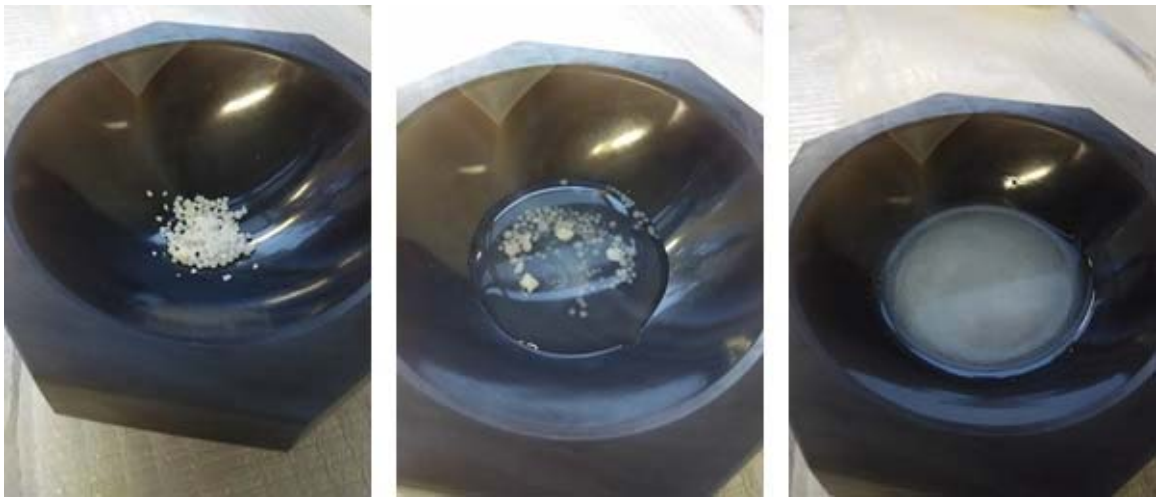

Impregnating Solution: Sn/C electrodes were generated by impregnating carbon with aqueous solutions of Tin (II) Chloride, Urea, and Water. Left: Urea and Tin (II) Chloride, Center: DI water added. Right: All species dissolved prior to impregnating carbon.

Figure 9. Precursor of Tin (II) Chloride, Urea, Water, and Carbon after Hand Grinding.

Impregnated Carbon. The solution is prepared to create a “paste like” consistency once it is mixed with the carbon, similar to “incipient wetness” concept employed for creating heterogeneous catalysts. Left: final mixture of Tin (II) Chloride /Urea/DI water and high surface area carbon. Right: Slurry in alumina boat prior to insertion into furnace for RES processing.

The paste is then heated in a flow of nitrogen of 100 standard cubic centimeters per minute (sccm) and brought to a temperature of 100 degrees Celsius for an hour to remove excess water. After heating for an hour at 100 degrees Celsius, the temperature is increased to 800 degrees Celsius while the flow rate of the nitrogen is reduced to 5 sccm. The furnace takes approximately four minutes to reach 800 degrees Celsius and is kept at 800 degrees Celsius for 30 seconds for the reduction-expansion process to take place (Figure 10).

Figure 10. Setup of Furnace with Heating in Inert Atmosphere.

Sample in furnace. The alumina boat/paste is loaded into a quartz tube, but placed outside furnace. After the tube is thoroughly flushed with N2 and heated to process temperature, the tube is moved such that the alumina boat is at center, as shown.

After the carbon and precursor mix is inserted into the preheated furnace and the temperature reaches approximately 650 degrees Celsius, a cloud of gases is observed

(Figure 11). This is a residue, mostly carbon, of the same decomposition process that produces the reducing species during the thermal decomposition of urea, which is typically above 600 degrees Celsius. In addition, the lowered flow of the nitrogen during this phase allows more time for the reduction gases to interact with the sample so as to produce more nucleation sites for the Sn atoms concomitantly produced by the decomposition of SnCl. Sn atoms bond to carbon radical species created in the carbon surface by the removal of surface oxygen groups creating Sn (metal) strongly bonded to the carbon surface (Figure 12).

Figure 11. Cloud of Gases Produced during Reduction Expansion Phase.

By-product formation. After the alumina boat/carbon paste is moved to furnace center, the urea in the paste decomposes at about 650 degrees Celsius, resulting in a cloud of decomposition product that freezes downstream. Left: Clean tube after insertion. Right: Tube after urea decomposes. Similar results reported earlier for RES production of metal particles.

Figure 12. Sample after Reduction Expansion Phase.

Sample after completion of RES. The sample tube is moved, such that the alumina boat is in a cool zone, exactly five minutes after the sample is inserted into the furnace. Shown: After about 30 minutes of cooling in flowing nitrogen, the fully formed electrode material is cooled and can be removed from the alumina tube.

c. Increasing the Tin Proportion vis-à-vis Tin Oxide

The activation of carbon support helped in producing pure tin in the samples created. However, the proportion of tin oxide was significantly higher than tin. This is undesirable as energy is better derived from Sn particles. Thus, the following series of experiments focused on removing the presence of oxygen and reducing the likelihood of tin oxides being formed.

(1) Using Ultrasound to Mix the Precursors

The first approach was to ensure that the Sn precursor would thoroughly mix with the carbon support. In this manner, Sn particles formed after reduction would be well distributed and less likely to oxidize after its formation. This was done in two stages. After hand grinding, the Sn precursor was subsequently placed in an ultrasonic bath for 20 minutes. Thereafter, the pre-treated carbon was added to the Sn precursor and placed into the ultrasonic bath for an additional 20 minutes (Figure 13). The heating process of the precursor remained the same as before.

Figure 13. Precursor Placed into an Ultrasonic Bath.

Ultrasound to improve mixing. In an effort to improve dispersion and produce smaller Sn particles various modifications to the process were tested. Left: After SnCl/urea/DI water paste was prepared, it was further treated in an ultrasonic bath. Right: Ultrasound treated precursor mixed with carbon and additional ultrasound treatment applied.

(2) Introducing Sn Precursor in an Inert Atmosphere

The second approach aimed to reduce oxygen being introduced into the furnace. Hence, the carbon was first heated at 600 degrees Celsius for ten minutes in air and subsequently at 950 degrees Celsius in an inert atmosphere under nitrogen gas flow. Separately, the Sn precursor was prepared and placed into a pipette. After the pre-treated carbon was cooled, the Sn precursor was pipetted into the carbon support within the quartz tube while maintaining the flow of nitrogen.

(3) Increasing the Proportion of Urea in the Precursor

The third approach aimed to reduce the presence of oxygen by increasing the amount of urea in the precursor. By doing so, it was theorized that more reducing gases would be formed and remove surface oxygens that remained on the carbon support. Instead of the ratio of 1:1 for tin (II) chloride: urea, the ratio was increased to 1:2. Carbon was heated in air, hand ground, and placed into the ultrasonic bath to be mixed with the Sn precursor as before.

d. Decreasing the Size while Maintaining the High Proportion of Tin Particles

Having tried diverse means to produce the desired tin/carbon electrode, the researcher shifted the focus of the study to the carbon support. It was theorized that large Sn particles were formed because the carbon support was coarse in nature. This meant that the Sn/surface radical ratio was too high to ensure small particle formation. However, with a finer carbon support, the Sn/surface ratio would be greatly reduced, allowing the number of Sn atoms forming at each “surface radical” to be smaller, allowing smaller particles to be formed. The experiment was repeated with the new carbon support of Vulcan XC72, a material with a far higher surface area per gram, heated in air followed by grinding only hand with the Sn precursor for ten minutes. The same heat treatment process was followed. This change in carbon support proved successful in producing the desired tin/carbon and these results are discussed in the subsequent chapter.

2. Aerosol Through Plasma

The ATP technique, invented by Phillips et al. [37], is a method by which precursors are passed through plasma and rapidly cooled to produce nanoparticles. It was found that when precursors of metallic particles and support material were passed through the plasma at >3000 degrees Celsius, the metallic particles atomized and rapidly cooled through a chimney and were deposited on a filter as nanoparticles on the support material (Figure 14). It is notable that the support was modified as well. In the case of a high surface area carbon, it is postulated that oxygen groups are removed, simply on the basis of the extreme temperatures achieved [38]. Moreover, there is clear evidence from other studies [39] that bonding sites may also be created. This allows metal to bond directly to carbon atoms on the surface of these sites.

Figure 14. Schematic of Aerosol Through Plasma (ATP) Technique.
Source: [37].

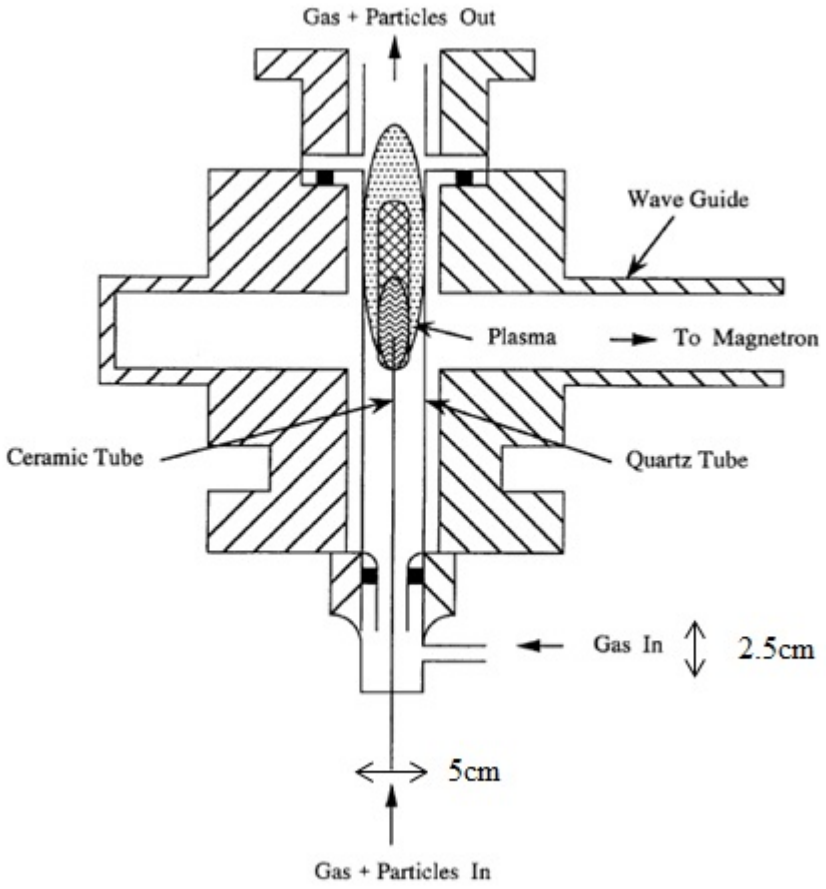

Aerosol Through Plasma (ATP) approach to production of Sn/C. In the ATP process the precursor is a dry mix of micron scale Sn particles. This mix is converted below the torch to an aerosol by rapid gas flow and agitation. The aerosol is passed through a hot plasma zone where the Sn is converted to a vapor, which is absorbed onto the carbon to form small particles. The particles freeze on the cool afterglow zone just above the torch. Shown: Cross section of the plasma zone.

In this series of experiments, 0.125g of micron-sized Sn were mixed with 0.5g of carbon as precursors. Argon at 30 sccm was passed through the system and carried the precursors past the 900W microwave-powered plasma at a fraction of a second. In order to keep the system closed without introducing oxygen, the pressure of the system was set at 748 Torr (Figure 15). As a reference, atmospheric pressure for the room was 738 Torr.

Figure 15. Setup of Aerosol-Through-Plasma (ATP).

ATP system. The plasma system. A) Power Supply, B) Magnetron, C) Wave guide, D) Chimney

Although the method required less effort in the preparation of the precursor, it required more time in ensuring that the system was safe for operation. Safety requirements such as wearing of goggles while plasma was in operation, wearing of thermal gloves for handling of the chimney, as well as radioactivity checks needed to be strictly adhered to (Figure 16). In addition, the process only produced approximately 0.01g of sample during the first iteration. Hence, the entire process took much longer to produce 1g of sample compared to RES.

Figure 16. Closeup of Plasma Torch.

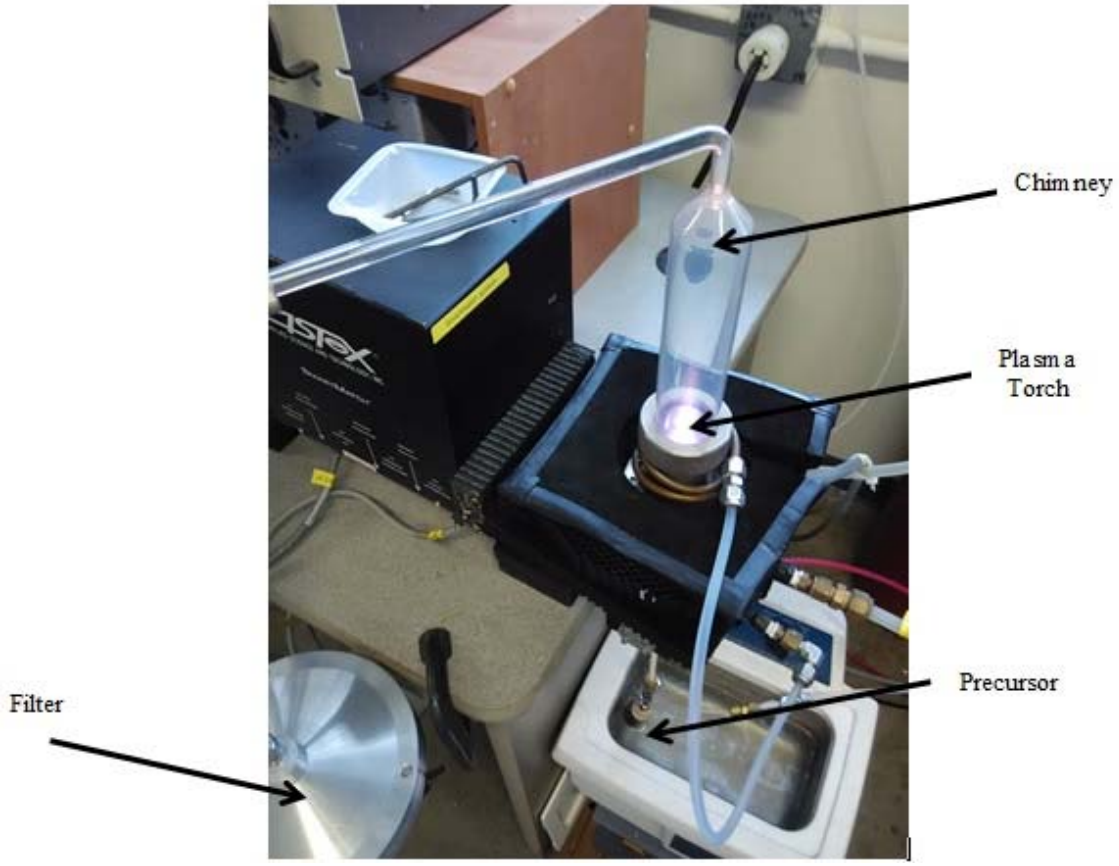

In the ATP process the precursor aerosol passes through the hot zone (approx. 0.1 s) where it is heated to about 3400 C, then into the afterglow inside the chimney where it cools. The completed material is captured on filter paper.

B. CHARACTERIZATION

This section will discuss the various methods used in characterizing the Sn/C sample created.

1. X-Ray Diffraction

X-ray diffraction was used to determine the identity of the crystalline phases present in the samples. XRD occurs when an X-ray is incident upon a crystalline material. The diffraction pattern can then be analyzed using the wavelength of the incident X-ray as well as the geometric arrangement of the atoms according to Bragg's Law. Bragg's Law is mathematically described by $n\lambda = 2d_{hkl}\sin\theta$ where, d_{hkl} is the

distance between crystallographic planes, n is order of reflection, and λ is wavelength of the X-ray, while θ describes the incident angle at which the diffraction peak occurs.

Figure 17. Rigaku MiniFlex 600 XRD.

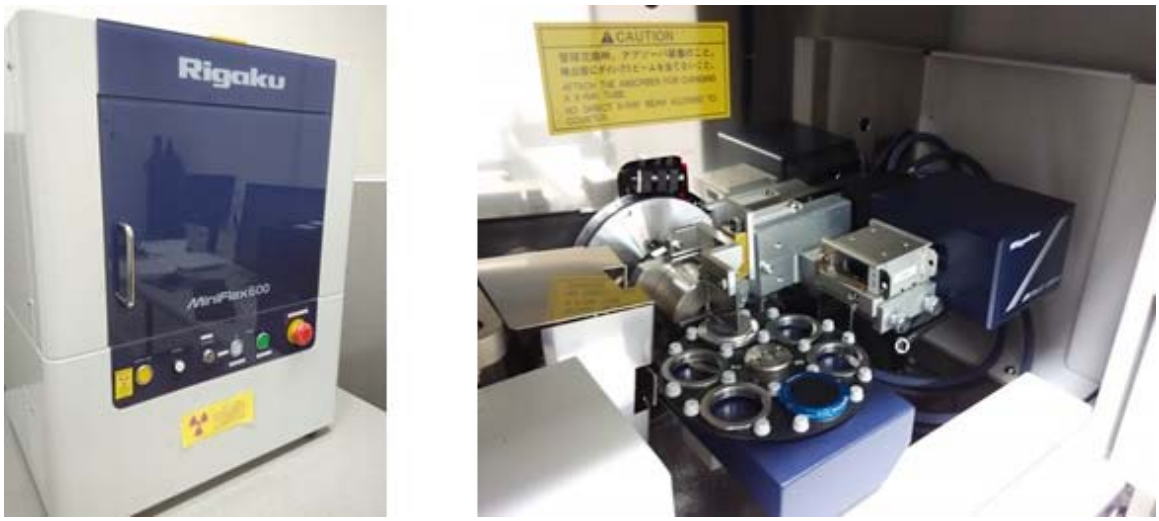

Left: Rigaku MiniFlex 600 XRD. Right: Sample placed inside XRD.

To carry out analysis, a small amount of the sample was transferred onto a sample holder and placed into the Rigaku XRD (Figure 17). Analysis conditions were set at 20kV, 2mA using a copper X-ray source of 1.54 angstrom. Within the Rigaku XRD, the sample was tilted from 10 degrees to 100 degrees (2θ) so as to capture a pattern for the desired sample. The pattern was then compared using an analysis program that has a database of known crystal spectra (Figure 18).

Figure 18. Example of XRD Pattern.

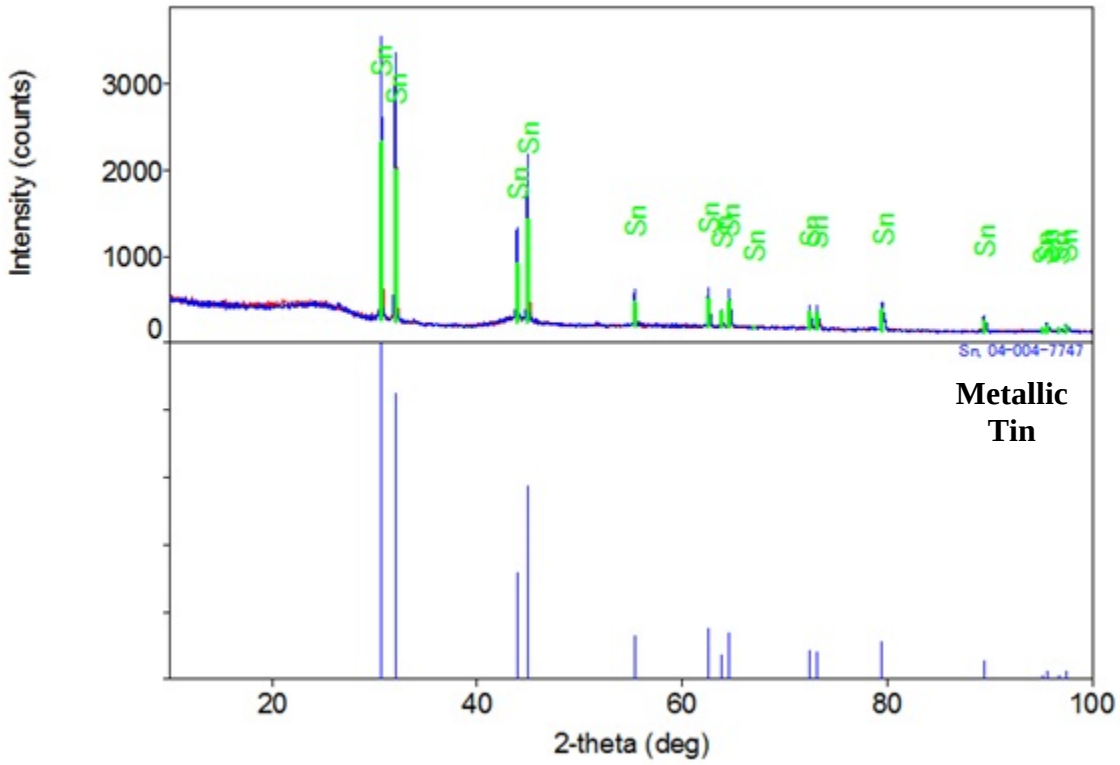

After the XRD pattern is collected it is interpreted using a library of species patterns. Shown: All lines in the XRD pattern of an ATP-produced electrode material are identified as metallic Sn.

Using the XRD pattern developed, an average particle size can be quickly estimated from the Debye-Scherrer Equation, given by $D = \frac{k\lambda}{\beta \cos\theta}$ where D is the particle size in nanometers (nm); k is the crystallite shape factor; λ is the wavelength of the X-ray in nm; β is the full width at half the maximum (FWHM) of the X-ray diffraction peak; and θ is the Bragg's angle. For standard practice, a shape factor of 0.9 is used for spherical nanoparticles [40].

2. Scanning Electron Microscopy / Energy Dispersive Spectroscopy

SEM was employed to determine the morphological features of the particles in the samples, and EDS the identity and distribution of the elements that compose the specimens (Figure 19). As the name suggests, the SEM uses a focused beam of electrons

to scan a sample and produce an image. EDS, on the other hand, uses a beam of energetic electrons to knock out the electrons from the shells of atoms within the sample. To fill these holes and minimize potential energy, electrons from higher energy states fill the holes, and in doing so, the electrons release a photon that corresponds to the energy difference between the two states (Figure 20). The energies of these photons (X-rays) are then characterized, providing the identity of the elements but not the true chemical state within the sample. Detectors within the SEM can localize the origin of the signal to within 1 angstrom (Å), enabling an approximate map of elements and element concentration to be generated. It will then monitor the signals from the energy and construct a greyscale image for display.

Figure 19. Zeiss NEON 40 SEM.

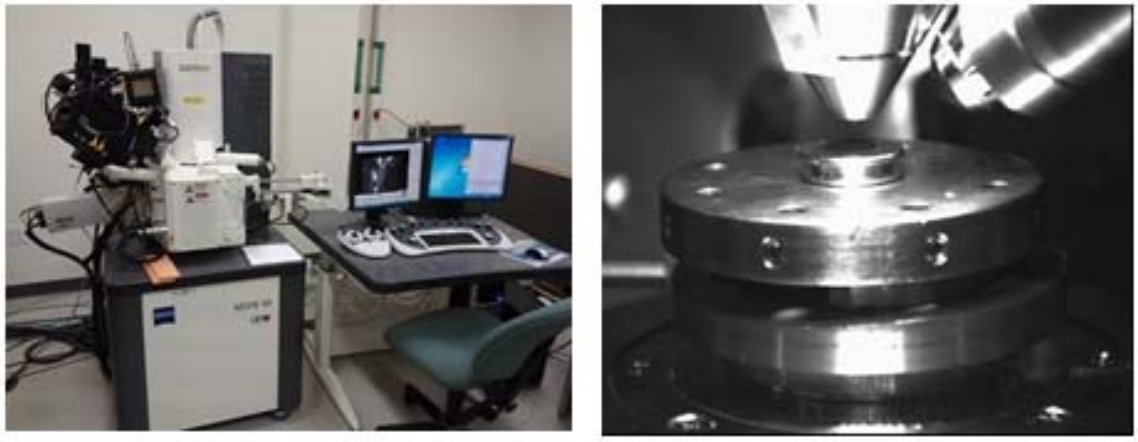

Setup of SEM. Left: SEM and movement of stage using joystick controls. Right: Sample placed in the center of the stage inside the SEM.

Figure 20. Example of SEM Image.

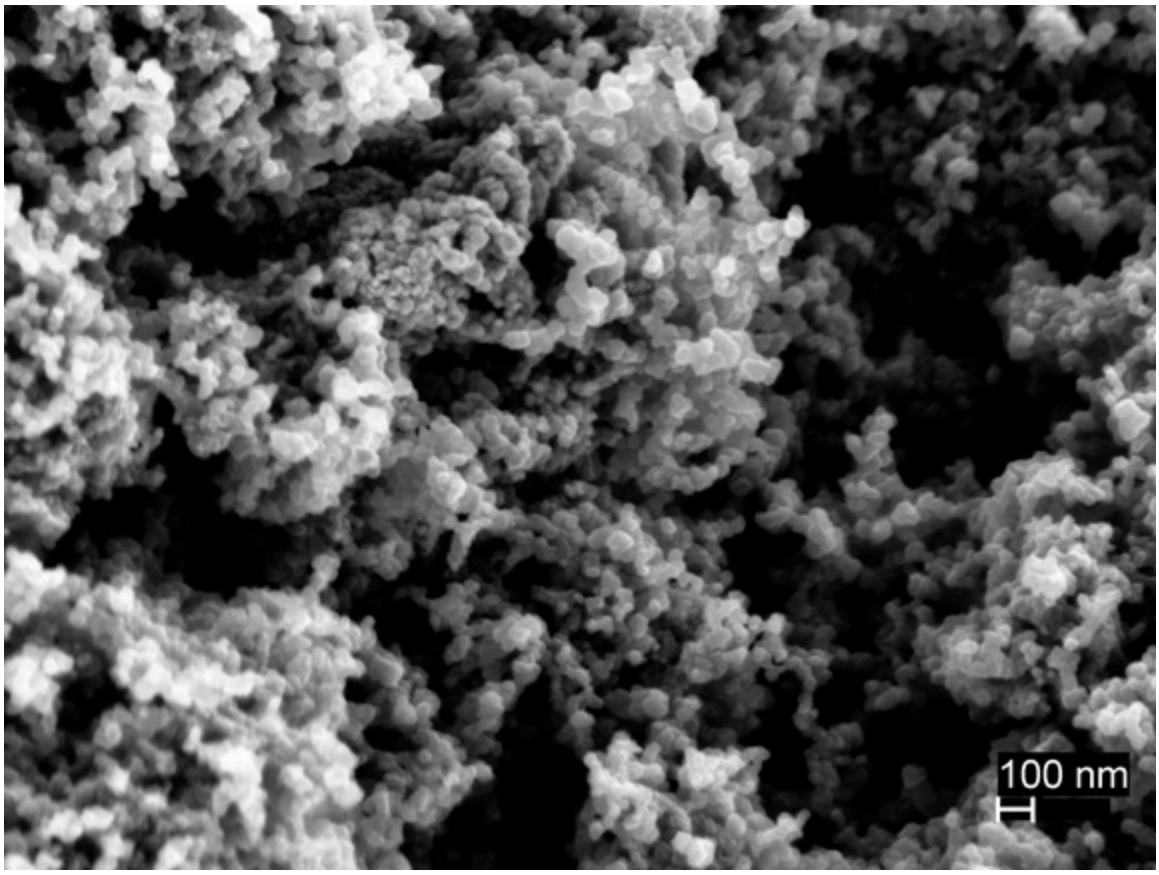

SEM capable of imaging particles in the order of nanometers. Shown: High surface carbon particles used in the study.

The Zeiss NEON 40 SEM was used to characterize the samples created using conditions of 2kV accelerating voltage and an aperture of $30\,um$. In addition to imaging the sample, EDS was also able to map the elemental composition and location within the sample (Figures 21, 22).

Figure 21. Example of EDS Image.
(Clockwise: Image, Carbon, Oxygen, and Tin.)

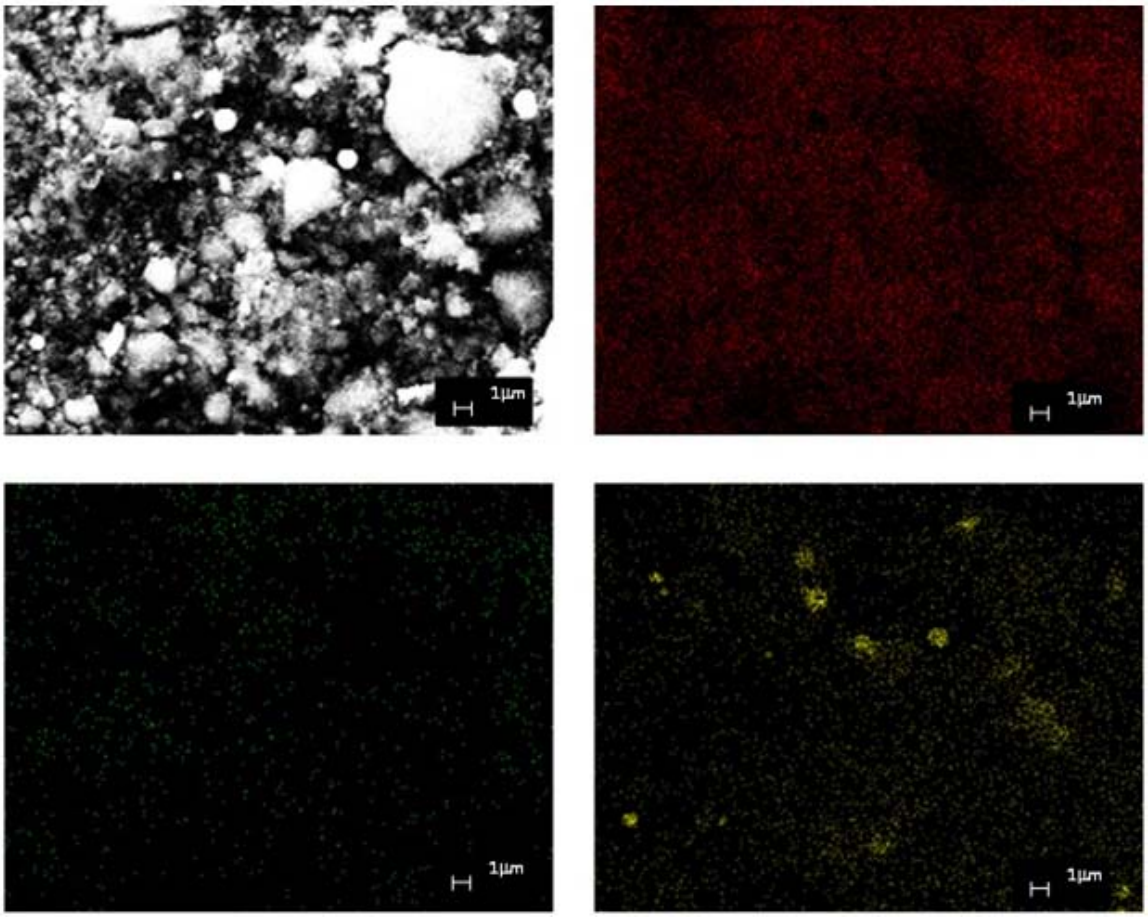

EDS Elemental Display. EDS is capable of showing the distribution of particles in the sample. By counting intensities of the elements in the sample and displaying them in different colors, the distribution within a sample can be easily seen. Top left (in clockwise direction): SEM image of Sn/C sample, Carbon Distribution (Red), Tin Distribution (Yellow), Oxygen Distribution (Green).

Figure 22. Example of EDS Pattern.

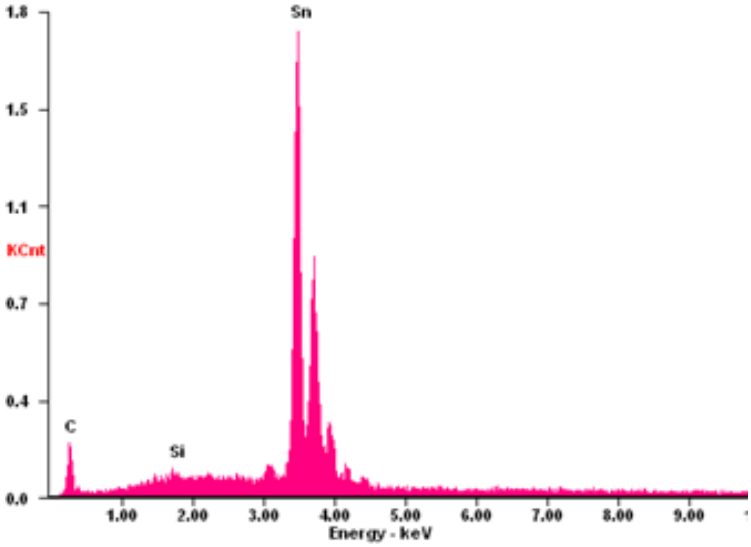

Intensities of elements within a sample can also be shown through a pattern. Shown: Sample containing Sn, C, and trace Si.

3. Transmission Electron Microscopy

Unlike SEM, where electrons are reflected off the sample, the TEM analysis is solely based on a beam of electrons that pass through the sample, thus allowing the observation of the internal features of the specimen under study. The number of electrons collected at each point is employed to create a grey scale image (Figure 23). Due to the shorter wavelength of the beam deployed by the TEM, it is able to reach resolutions that are 100 times higher than SEM. This allows the TEM to analyze samples in the order of angstroms.

Figure 23. TEM and an Example of TEM Image.

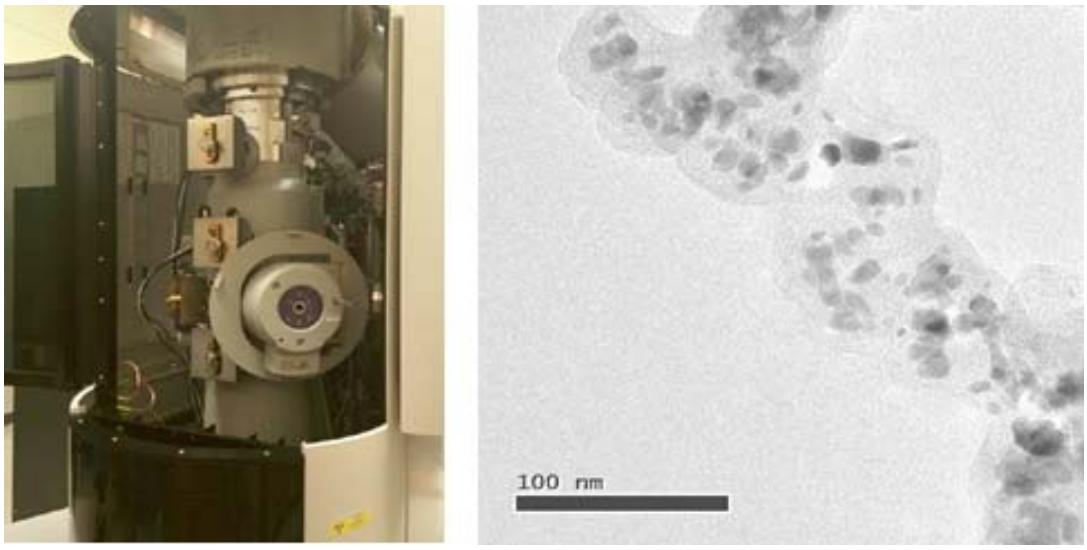

TEM Imaging Left: Tecnai Osiris TEM at the Naval Postgraduate School. Right: Bright field image produced by TEM showing Sn/C sample where Sn is encapsulated in carbon support.

Although the size of the particles as determined by SEM was in the order of nanometers, it was TEM that provided the resolution in confirming the size and distribution of the Sn particles. The TEM is equipped with EDS analysis, similar to the one used in the SEM.

Information from XRD, SEM, and TEM helped to confirm initial hypotheses and shaped subsequent approaches. These are discussed in the next chapter. A description of all experiments carried out during this study is provided in the Appendix.

THIS PAGE INTENTIONALLY LEFT BLANK

III. RESULTS

This chapter describes the results from each stage of this study. Experiments were carried out to determine the temperature at which dangling bonds would be created on the carbon surface, prevent the formation of tin oxides as well as minimize the size of the tin metal particles. The results of these experiments are discussed in this chapter.

A. ACTIVATING THE CARBON SUPPORT

As described in the experimental methods, the Sn precursor, urea, and water were mixed with untreated high surface area carbon and heated to 800 degrees Celsius under an inert atmosphere. In order to create a high energy form of tin/sodium or tin/lithium, pure Sn particles of nanometer (nm) dimensions should be found on the carbon support. However, the XRD pattern for the first three experiments showed that only tin oxide was present as Sn usually found at ~33 degrees was absent (Figure 24).

Figure 24. XRD Pattern of Sample without Activated Carbon.

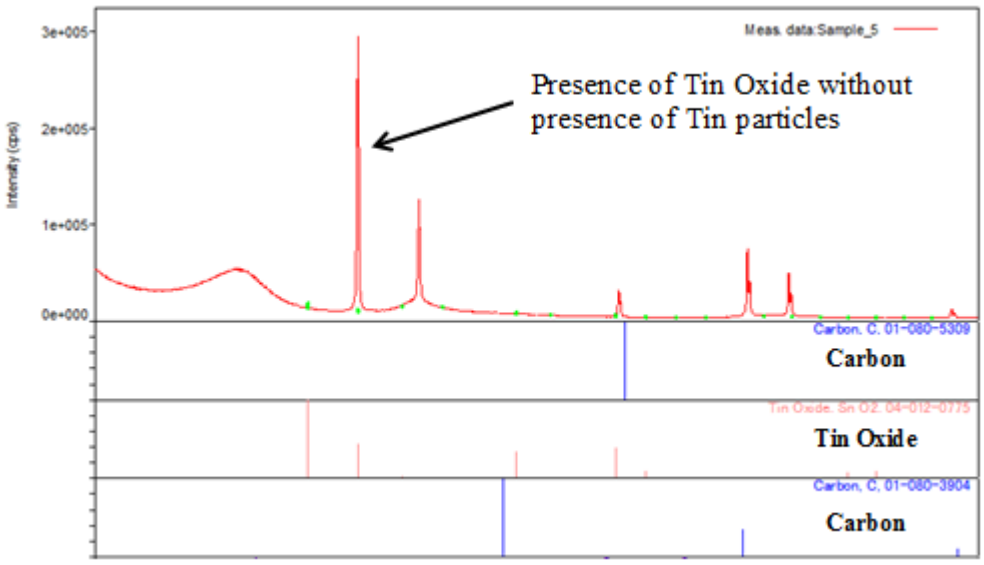

Without the use of activated carbon, strongly bonded Sn/C linkages were absent. Instead carbon-oxygen-tin linkages were formed, resulting in the presence of tin oxides. Notably, the presence of pure Sn particles was absent.

This prompted a closer look at the pre-treatment of the carbon support in order to produce activated carbon. It was found that the heating of the carbon support is important to the entire approach for the following reasons:

- The carbon without any heat treatment is hydrophobic. This means that the carbon repels and does not mix with the Sn precursor. This was verified when a drop of water was dripped on top of the carbon support. Instead of being absorbed, the water formed spherical particles over the surface of the carbon, indicating the hydrophobic nature of the untreated carbon.
- The heating of the carbon is also important in creating active sites on the surface of the carbon. Upon heating in air, oxygen molecules adhere to the surface of the carbon. The oxygen molecules are subsequently removed during the reduction process to form dangling carbon bonds whereby a strong linkage between the Sn (from the Sn precursor) and the carbon can be formed.

However, if carbon is heated for an excessive time and temperature, it will form carbon dioxide and is lost to the surroundings. Hence, the next series of experiments proceeded to determine the optimal time and temperature to heat the carbon. The parameters are described in Table 1:

Table 1. Parameters for Heating of Carbon Support.

Run	Duration (min)	Temperature (degrees Celsius)	% weight loss
1	60	750	
2	60	700	No carbon remained
3	60	650	59
4	60	600	36
5	10	675	59
6	30	600	41
7	10	600	11

Initial heating parameters left no trace of carbon. Hence, duration and temperature were decreased to obtain an optimal weight loss of 11% to activate carbon. Carbon was eventually activated by heating at 600 degrees Celsius for ten minutes to allow oxygen groups to attach to the surface of the carbon support.

Results showed that carbon forms carbon dioxide at temperatures higher than 700 degrees Celsius. In addition, at a lower temperature of 675 degrees Celsius, even for a

short duration of minutes, weight loss was at 59%. The parameters of 600 degrees Celsius and ten minutes heating time was finally decided upon as the 11% weight loss indicates that active sites have been created without a significant loss of carbon. This was the carbon pre-treatment protocol used for the rest of the experiments.

The first breakthrough occurred after determining the pre-treatment of carbon. It was found that using pre-treated carbon or activated carbon, with all other parameters remaining the same, the resultant sample produced not only a sample with tin oxide as before, but also a small presence of pure Sn (Figure 25). This was also verified through XRD, EDS, and TEM (Figures 26, 27). However, the proportion of Sn relative to tin oxide is relatively small.

Figure 25. XRD Pattern of Sample with Activated Carbon.

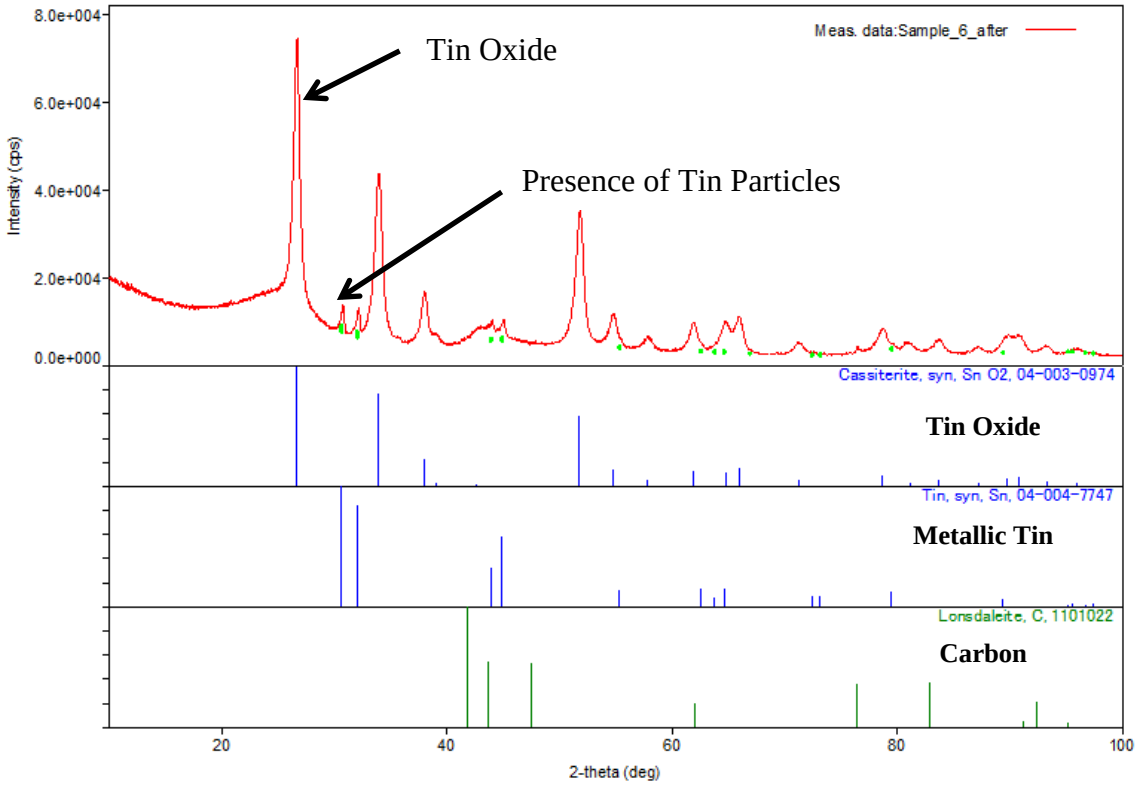

Result of activated carbon used in RES process. Due to direct linkage between Sn and C on the surface of the activated carbon support, presence of pure Sn particles was detected using XRD. However, the proportion of tin oxide is much higher than the proportion of pure Sn particles.

Figure 26. SEM Image at 5000x and EDS Indicating Presence of Tin Particles.

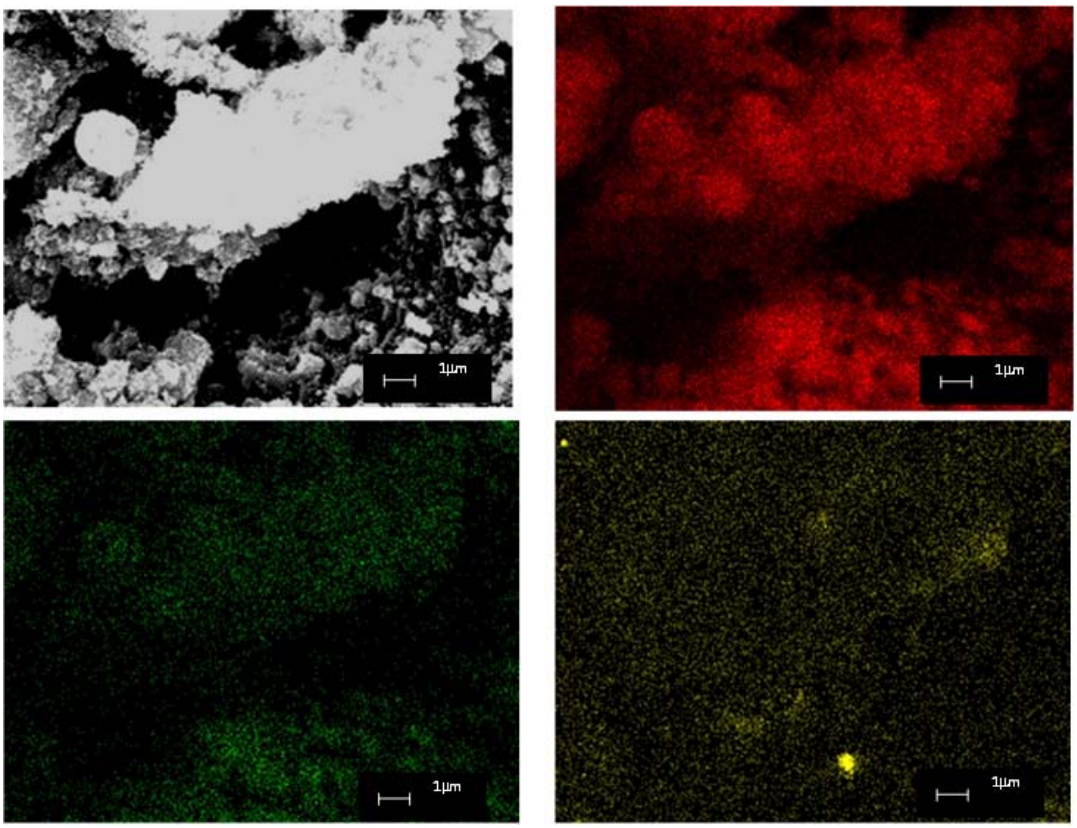

EDS Elemental Display of Sn/C after RES process using activated carbon and a nominal 10% Sn loading. Presence of small particles of Sn was found in the sample. Top left (in clockwise direction): SEM image of Sn/C sample, Carbon Distribution (Red), Tin Distribution (Yellow), Oxygen Distribution (Green).

Figure 27. TEM Images Indicating Presence of Tin Particles.

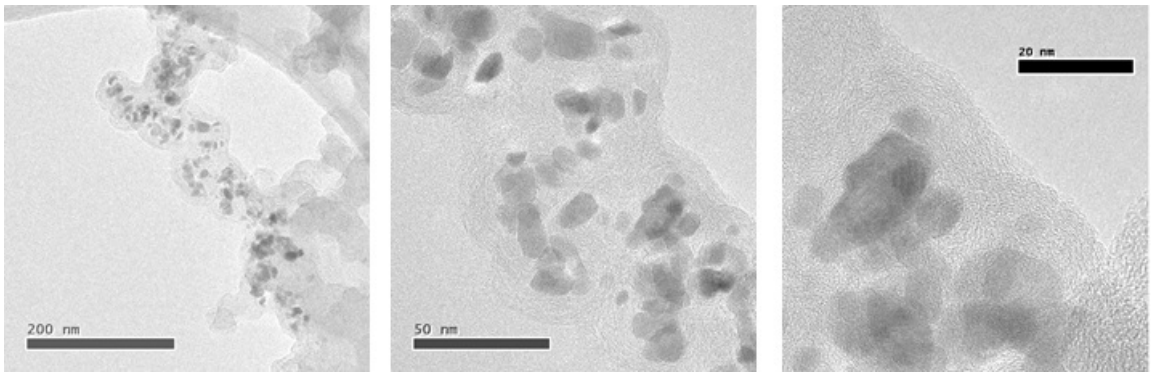

TEM characterization of RES protocol, 10 wt % Sn on activated carbon support. Bright field imaging shows Sn particles on the carbon support. Sn particles are also shown to be small, in the order of 20 nm.

B. INCREASING THE PROPORTION OF TIN PARTICLES RELATIVE TO TIN OXIDE

With the successful fabrication of a sample with nanoscale tin metal particles on the carbon support, the next phase of experiments focused on increasing the proportion of Sn particles and decreasing the size of the particles. This is because Sn particles and not tin oxide are required in the operation of a tin/lithium battery. In addition, it is also postulated that smaller Sn would serve to reduce the effects of volume expansion of Sn particles that occurs during lithiation.

1. Using Ultrasound to Mix the Precursors

As described in the experimental methods, ultrasound was used to mix the precursor in addition to hand grinding. The ultrasound serves to better distribute the tin precursor throughout the carbon support which allows more nucleation sites to be formed on the surface of the carbon support. It was found that the proportion of tin particles relative to tin oxide indeed increased after the ultrasonic process (Figure 28). This is an improvement as compared to the small proportion of tin relative to tin oxide previously (Figure 25). However, the presence of coagulated tin particles in the form of spherical particles (Figure 29) showed large tin particles in the order of microns.

Figure 28. XRD Pattern of Sample after Ultrasonic Process.

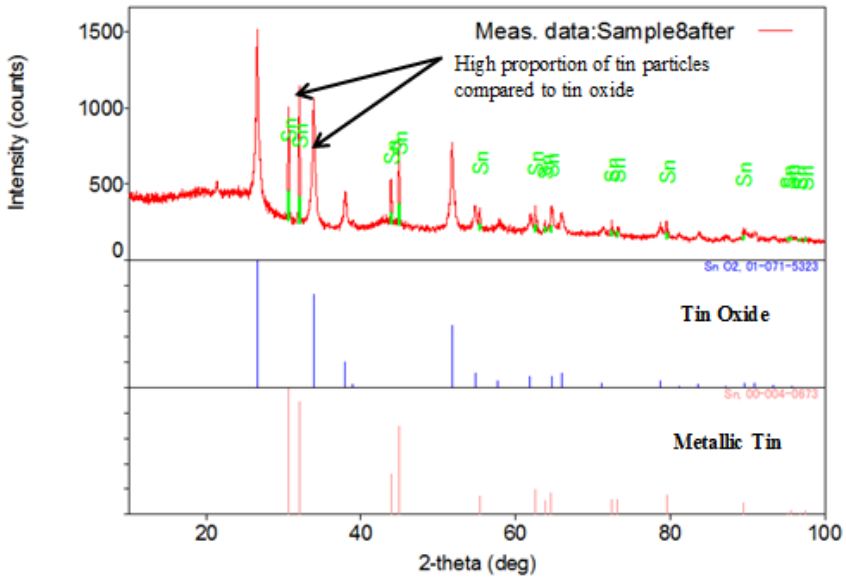

Result of ultrasonic mixing of precursor. Ultrasonic mixing distributed the Sn precursor well in the carbon support. This resulted in more nucleation sites and thus a significantly higher proportion of pure Sn particles than previously seen (e.g., Figure 25).

Figure 29. Presence of Spherical Particles with Sizes in the nm and Micron Scales.

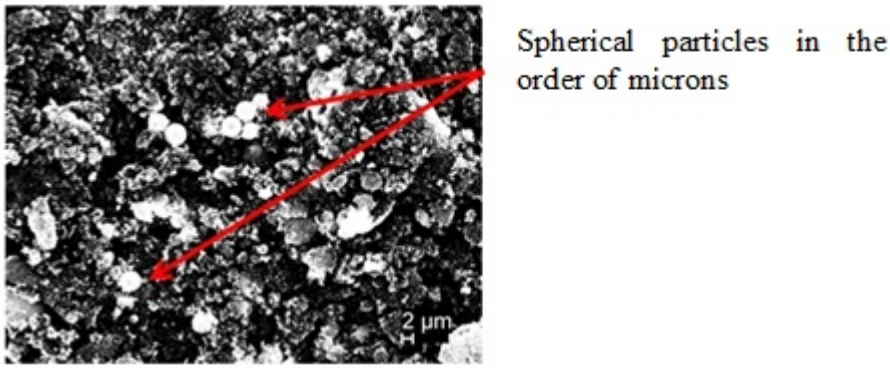

Although pure Sn particles are produced, micron-sized Sn particles are susceptible to crumbling and disintegration when cycled in a battery. Shown: micron-sized Sn particles produced with ultrasonic mixing of Sn/C precursor.

2. Introducing Sn Precursor in an Inert Atmosphere

In addition to the use of ultrasound for mixing, two other methods were explored to reduce the amount of oxygen in the sample. First, the Sn precursor was introduced to

the carbon support in an inert atmosphere. This prevents the introduction of oxygen during the mixing of the Sn precursor and carbon support. Second, the proportion of urea in the precursor was increased. This helps to better remove carbon surface oxides during the reduction phase.

As described in the experimental methods, the Sn precursor was introduced to the carbon support via a pipette, in an inert atmosphere. Results showed that no tin oxide was observed (Figure 30). This demonstrated that the presence of oxygen (and thus oxides) could be eliminated in this manner. However, as the Sn precursors could not be mixed with the carbon in an inert atmosphere, the top of the sample presented a higher proportion of tin particles as compared to the lower portions. This meant that the tin particles were not as well distributed and were not able to reach all parts of the carbon support. The secondary effect of the poor distribution was that more tin atoms were present at each nucleation site, resulting in larger tin particles.

Figure 30. XRD Pattern of Sample Introducing Sn Precursor in an Inert Atmosphere.

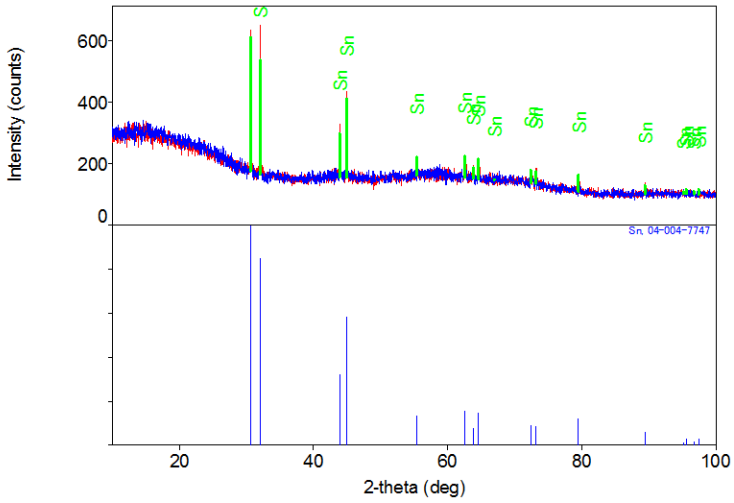

To reduce the presence of oxygen during the mixing of the precursors, the Sn/C solution was pipetted unto activated carbon in an inert atmosphere. This proved successful in producing pure Sn particles as shown in the XRD pattern.

3. Increasing the Proportion of Urea in the Precursor

The second approach, aimed at reducing the presence of oxygen, was done by increasing the amount of urea in the precursor. With the increased amount of urea, more reducing gases would be released, and with it, the oxygen on the surface of the carbon support can be removed. Instead of the ratio of 1:1 for tin (II) chloride: urea, the ratio was increased to 1:2. Carbon was heated in air, hand ground, and placed into the ultrasonic bath to be mixed with the Sn precursor as before. The result showed that although not all of the oxides were removed, the proportion of tin particles relative to tin oxides was dramatically increased (Figure 31). However, many tin particles remained in the order of microns in size (Figure 32).

Figure 31. XRD Pattern of Sample with Increased Proportion of Urea.

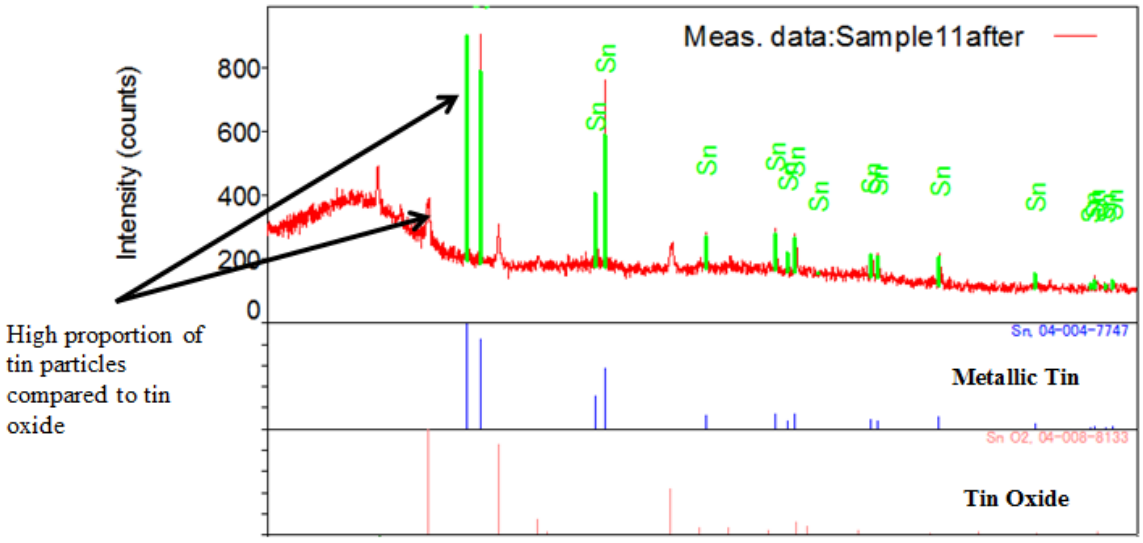

Result of increasing Urea/Sn ratio. Increasing the ratio of urea served to remove excess surface oxides that remained on the carbon support. This resulted in the production of Sn/C with high proportion of pure Sn compared to production with a lower urea/Sn ratio (Figures 25 and 28) as compared to tin oxide as shown here.

Figure 32. SEM Image of Sample with Increased Proportion of Urea.

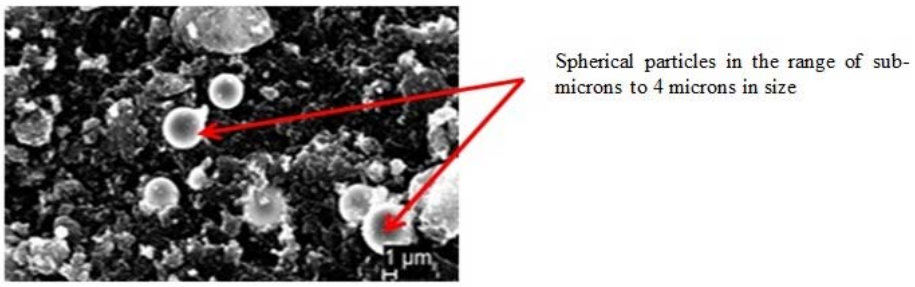

Although pure Sn particles are produced using the increased ratio of urea, micron-sized Sn particles are still present. These are undesirable as larger sized particles are susceptible to crumbling and disintegration when cycled in a battery.

C. DECREASING THE SIZE WHILE MAINTAINING THE HIGH PROPORTION OF TIN PARTICLES

While there was success in producing samples that consisted primarily of nano-scale tin particles with oxides, as well as samples with high proportion of metallic tin particles on separate occasions, there was no sample that had both. Having exhausted methodical means of achieving the desired outcome, this researcher shifted the focus of the experiments to the carbon support. It was postulated that a different carbon support, one with higher surface area, would have more nucleation sites, thus smaller tin particles would form. Hence, the study moved on to focus on a different carbon support—Vulcan XC72. This carbon had higher surface area and was composed of very fine particles in the range of 30 and 60 nm. The experiment was repeated with the new carbon support heated in air followed by only hand grinding (without ultrasonic bath) with the Sn precursor for ten minutes. The same heat treatment process was followed.

While the XRD pattern showed a high intensity of tin particles (Figure 33), the EDS showed good distribution of tin particles (Figure 34), even at 20000X magnification, indicating the presence of nanoparticles. In addition to verifying particle size via TEM, the RES method has been demonstrated to yield successful results in producing tin nanoparticles and eliminating the presence of tin oxide. In particular, TEM results showed remarkably small Sn particles (2 nm average) created using the Vulcan XC72 carbon support. These were verified with both dark field and bright field images (Figures 35, 36).

Figure 33. XRD Pattern of Sample with Vulcan XC72 Carbon Support.

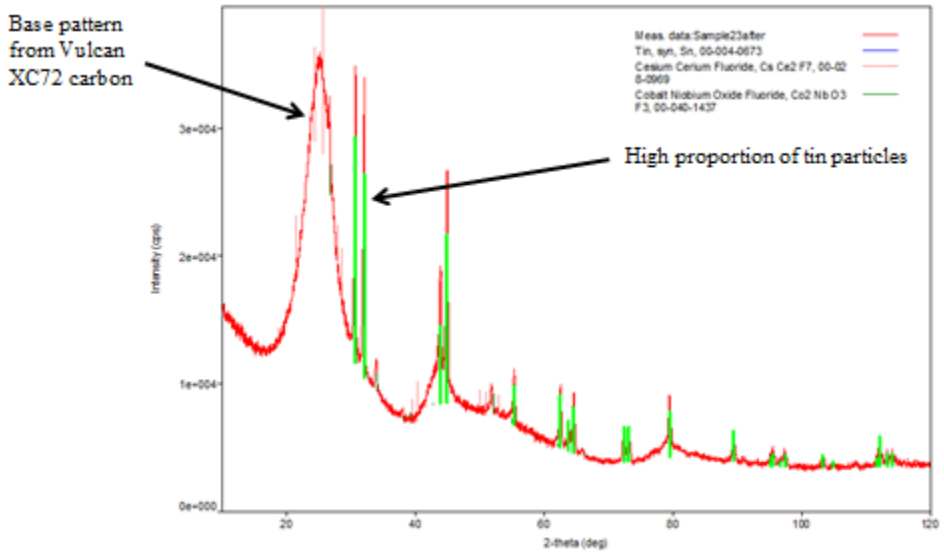

Result of using high surface area Vulcan XC72 carbon support. XRD results showed significantly high proportion of tin particles. The tin particles were calculated, using the FWHM of the peaks in the XRD as well as the Debye-Scherrer equation, to be approximately 30 nm in size.

Figure 34. SEM Image and EDS at 5000X Indicating Presence of Tin Particles.

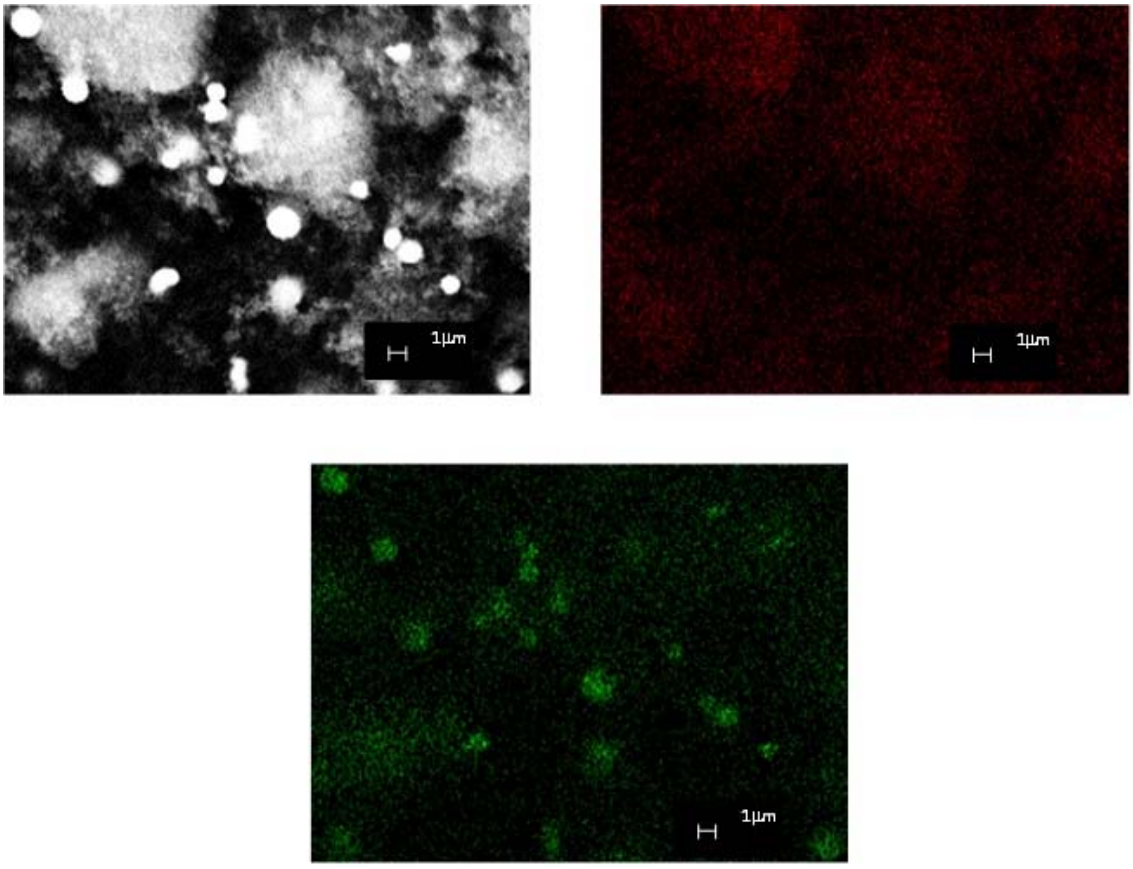

EDS Elemental Display. Although spherical Sn particles are still identified, EDS also shows distribution of Sn throughout the carbon support, suggesting presence of much smaller Sn particles. Top left (in clockwise direction): SEM image of Sn/C sample, Carbon Distribution (Red), Tin Distribution (Green).

Figure 35. TEM Dark Field and Bright Field Image at 900000X.

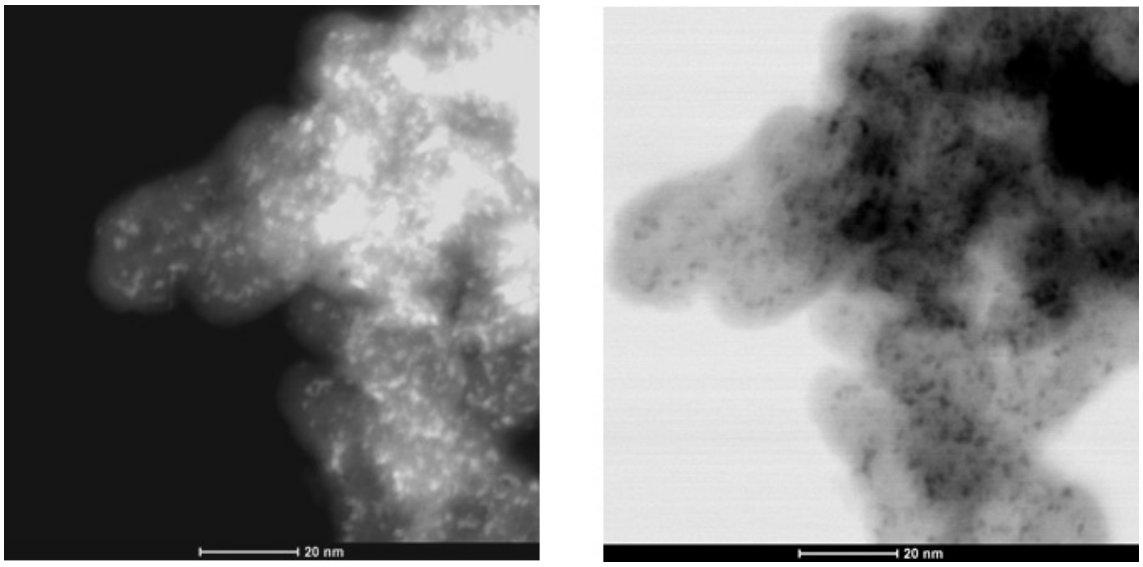

Result of TEM characterization of Sn/C formed with activated high surface area Vulcan XC72 carbon support. Dark Field (left) and Bright Field (right) imaging at 900kX showing presence of remarkably small Sn particles, in the order of 2 nm.

Figure 36. TEM Dark Field and Bright Field Image at 1250000X.

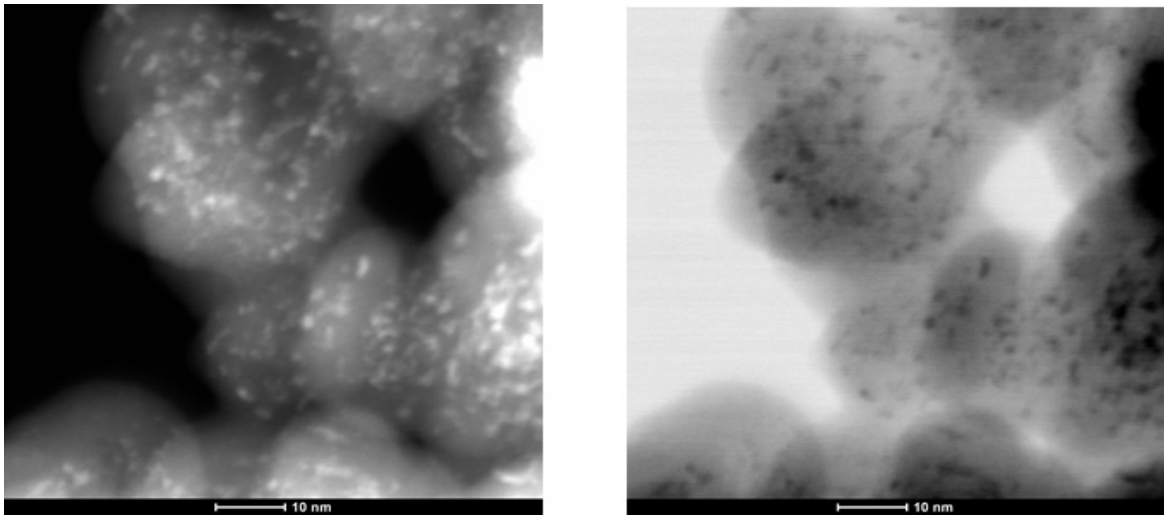

Result of TEM characterization of Sn/C formed with activated high surface area Vulcan XC72 carbon support. Dark Field (left) and Bright Field (right) imaging at higher magnification of 1250kX showing the presence of remarkably small Sn particles (in the order of 2 nm)

D. INCREASING THE TIN PROPORTION TO 20%

The Sn/C sample created in the previous section contained 10% tin by weight. To better study the energy density of the Sn/C electrode, a sample that contained 20% of tin was created. The sample created was subsequently characterized using XRD (Figures 37, 38), SEM, and EDS (Figure 39).

Figure 37. XRD Pattern of Sample with 20% Tin Loading.

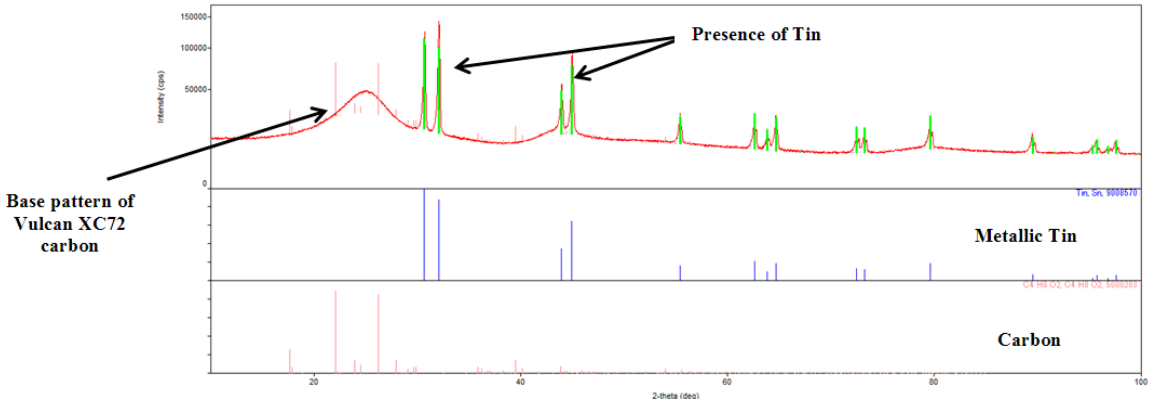

XRD characterization of 20% tin loading Vulcan XC72 Sn/C sample. Sn/C created with 20% loading of tin by weight showing presence of pure Sn particles. Increase of tin loading to 20% produced a similar XRD pattern as that of 10% loading Sn/C, suggesting potential of further increase in tin loading.

Figure 38. XRD Pattern of Sample Showing Increased Intensity of Tin.

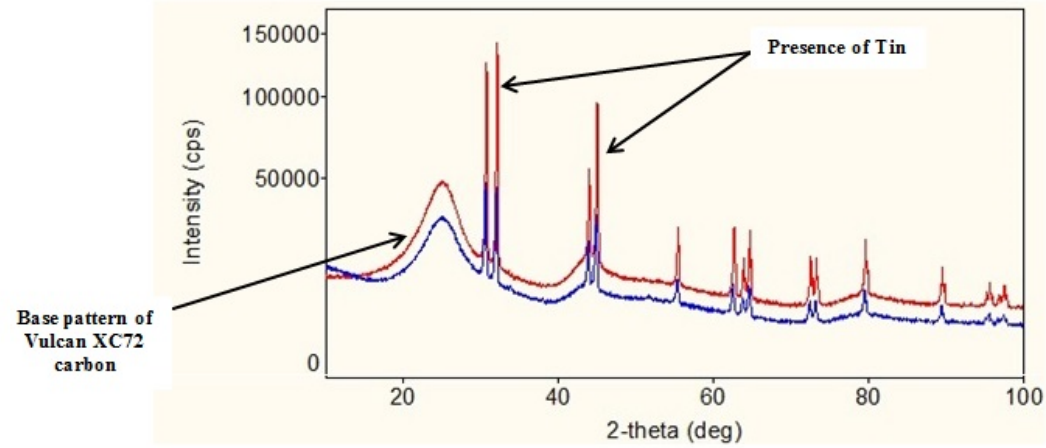

Comparison of XRD pattern of sample prepared on Vulcan XC72 between 10% and 20% tin loading of Sn/C. Pattern in red shows 20% Sn/C sample having higher intensity of Sn as compared to 10% Sn/C sample.

Figure 39. SEM Image and EDS (C, Sn) Showing Well Distributed Sn Particles.

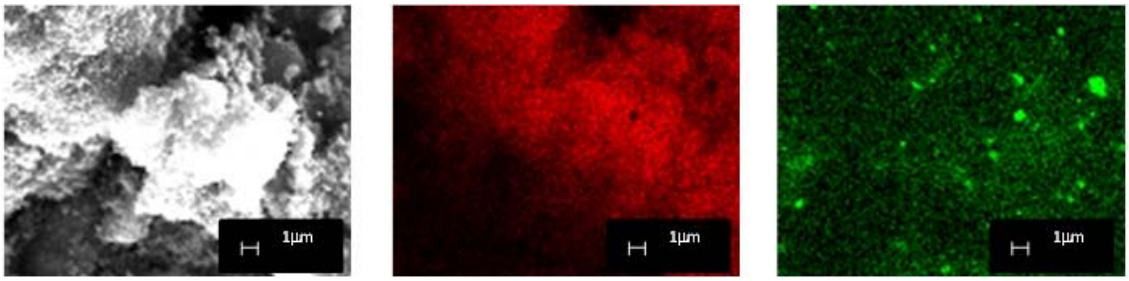

EDS elemental display of 20% tin loading on Sn/C sample prepared on Vulcan XC72. EDS showing presence of well distributed Sn particles that are in the order of nanometers. Left: SEM image of 20% Sn/C. Center: Carbon Distribution (Red). Right: Tin Distribution (Green).

XRD results showed that pure Sn particles were present (Figures 37, 38). In addition, EDS results (Figure 39) also demonstrated that the Sn particles were well distributed on the carbon support.

After the fabrication of both the 10% and 20% tin loading Sn/C electrode, the next step in the study was to determine the performance of the Sn/C electrode in a battery cell.

E. PERFORMANCE OF MATERIAL IN A BATTERY

Both the Vulcan XC72 10% and 20% Sn loading samples were sent to Purdue University for tests in a battery half-cell. The following section describes the method that was used as well as its results. The electrochemical characterization process was described by Graduate Research Assistant Ryan Adams from the lab of Professor Vilas Pol in the Chemical Engineering Department of Purdue University.

1. Electrochemical Testing Parameters

Laminates were made by taking 80 % wt. of the sample, 10% wt. conductive additive (Timcal Super C65), and 10% wt. polymeric binder (polyvinylidene difluoride) on copper current collector. A slurry was formed utilizing N-methyl-2-pyrrolidone (NMP) as solvent and mixed for 20 minutes before applying it to a copper foil. After drying for 12 hours in a vacuum oven set to 80°C, electrodes with a diameter of 12 mm were punched out (active material loading ~ 1.5 mg cm-2).

Coin cells (2032 type) were assembled in an Argon atmosphere (99.998%) high purity glovebox. For Li-ion half cells, lithium metal foil was used as the counter electrode, with 1.0 M LiPF6 in ethylene carbonate/diethyl carbonate/dimethyl carbonate + 3% fluoroethylene carbonate additive as electrolyte and Celgard 2500 as separator. For Na-ion half cells, sodium metal foil was used as the counter electrode, with 1.0 M NaPF6 in ethylene carbonate/diethyl carbonate + 3% fluoroethylene carbonate additive as electrolyte and Whatman glass fiber as separator. Cyclic voltammetry was performed at a scanning rate of 1 mV s-1 utilizing a Gamry 600+ instrument. All galvanostatic cycling was conducted with an Arbin cycler, with current densities ranging from 20 – 500 mA g-1 in a voltage range of 0.005 – 1.5 V vs. either Li+/Li or Na+/Na. In addition, the effect of fluoroethylene carbonate (FEC) as electrolyte additive was tested to see if it was able to accommodate volume expansion with Sn nanoparticles.

2. Results of Battery Tests

The sample was cycled with both lithium and sodium while tested with the addition of FEC. The following figures show the capacity and energy of 10% Sn/C, 20% Sn/C, and carbon cycled in lithium-ion and sodium-ion battery cells (Figures 40, 41).

Figure 40. Discharge Capacity of Sn/C Li-ion Battery.

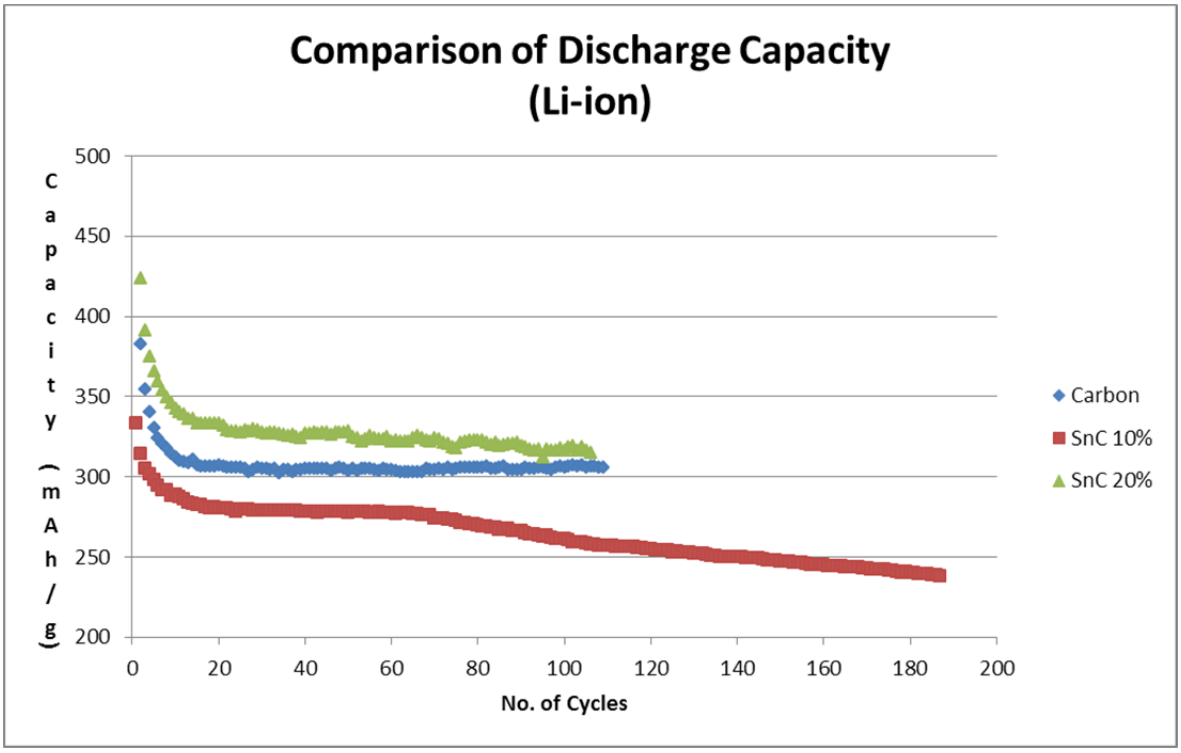

20% Sn/C is observed to have higher capacity value as compared to 10% Sn/C. The 320 mAh/g is approximately 18% higher than the 280 mAh/g demonstrating potential for higher capacity with further increase in tin loading. This demonstrates the participation of Sn during lithiation and its ability to remain stable in excess of 100 cycles. The higher discharge capacity of pure carbon compared to 10% Sn/C sample suggests Sn is prevented from participating in lithiation below a certain threshold. The low (below carbon) net capacity is consistent with only the Sn, which makes up only 10% of the electrode, participating in lithiation.

Figure 41. Discharge Capacity of Sn/C Na-ion Battery for Sn/C (10%).

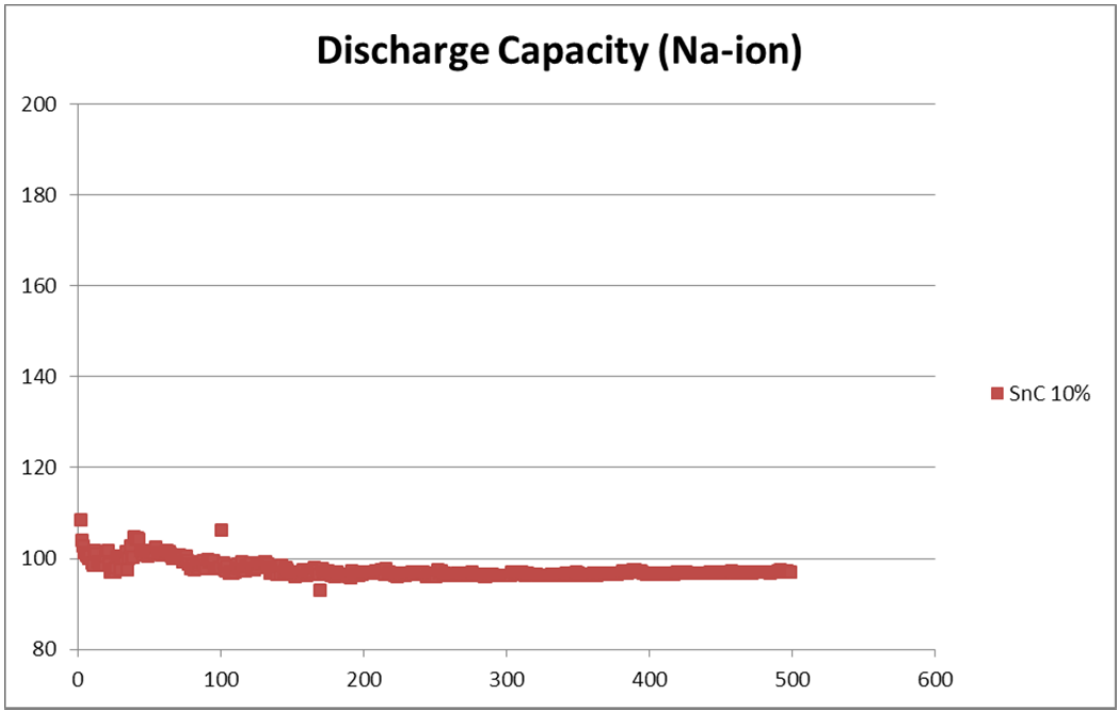

Discharge Capacity of Sn/C cycled in a Na-ion battery. Stability is demonstrated after Sn/C is cycled in a sodium battery for 500 cycles. This shows remarkably stable linkages between tin and carbon using RES, compared to crumbling of Sn that usually takes place after less than 25 cycles [41].

3. Proposed Sn/C Capacity Model

From the results, it can be seen that there is a critical amount of Sn below which a pure carbon sample will have a higher capacity as compared to an Sn/C sample. Hence, it is postulated that during the cycling process, lithium interacts with both Sn and C on the Sn/C electrode. However, due to the presence of Sn, below the critical amount, lithium interaction with carbon is reduced. Nonetheless, given the results of the 10% and 20% Sn loading data, an Sn/C capacity model is proposed according to the formula shown in Figure 42.

Figure 42. Proposed Formula for Sn/C Sample.

$$Capacity\ \left(\frac{mAh}{g}\right) = \frac{Weight\ of\ Carbon}{Total\ Weight} \times 180\,\frac{mAh}{g} + \frac{Weight\ of\ Tin}{Total\ Weight} \times 800\ \frac{mAh}{g}$$

The proposed formula (Figure 42) is a preliminary model that describes the capacity of Sn/C samples produced via RES. However, it is noted that two data points may be insufficient to draw an accurate model at this juncture. Further work is required to test the actual capacity with increased tin loading to further refine the proposed model.

Figure 43 shows the results of doubling the tin loading from 10% to 20%. There is a marked (approximately 18%) increase in the specific capacity with the increased tin loading. It is also noted that the specific capacity for the Sn/C Li-ion battery is very near to the ideal specific capacity of carbon. As Vulcan XC72 carbon is a commonly accessible carbon, the specific capacity again points to participation of Sn during lithiation. In addition, the sample with increased loading has been cycled for more than 100 cycles, and that stability is seen particularly for the Sn/C Na-ion battery, which has an 500 cycles (Figure 41). Future work with regard to this finding is discussed in the conclusions section.

Figure 43. Comparison of SnC23 (10% Sn) vs. SnC29 (20% Sn) Cycled in Li-ion Battery.

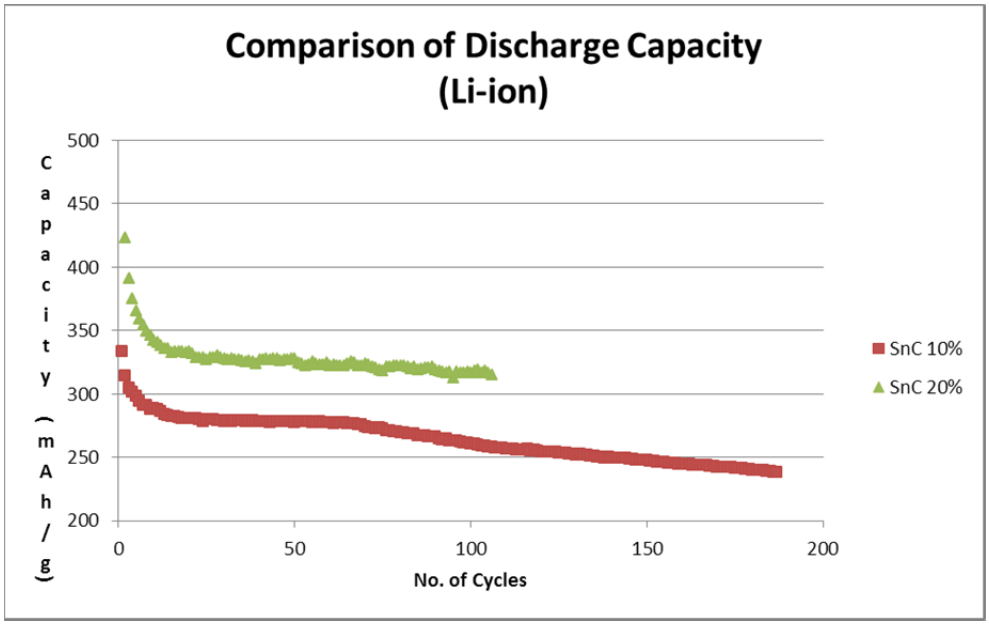

Comparison of discharge capacity between 10% and 20% tin loading on Sn/C. Note that 20% Sn/C has an approximately 18% higher discharge capacity compared to 10% Sn/C. This suggests potential to further increase discharge capacity with further increase of tin loading.

Figures 44 and 45 show post-cycled TEM images of Sn/C Li-ion and Sn/C Na-ion samples, respectively. Interplanar spacing calculations show the presence of tin oxide after more than 100 cycles. Although TEM results show tin oxide, it is postulated that Sn was present after cycling but oxidized prior to characterization under TEM. Verification via XRD (Figure 46) showed the presence of Sn metal after cycling in a battery, adding to the postulation that Sn remained after cycling but was oxidized due to the remarkably small nature of the Sn particles. In addition, the FWHM (Figure 47) of the tin peak showed extremely small particle sizes in the order of 10 nm. This meant that the Sn particles remained largely unchanged even after extended periods of cycling. However, due to the small amount of post-cycled material received from Purdue University, further analysis of future samples would better aid the presentation of the data.

Figure 44. TEM Images of Sn/C Li-ion Battery (Post Cycling).

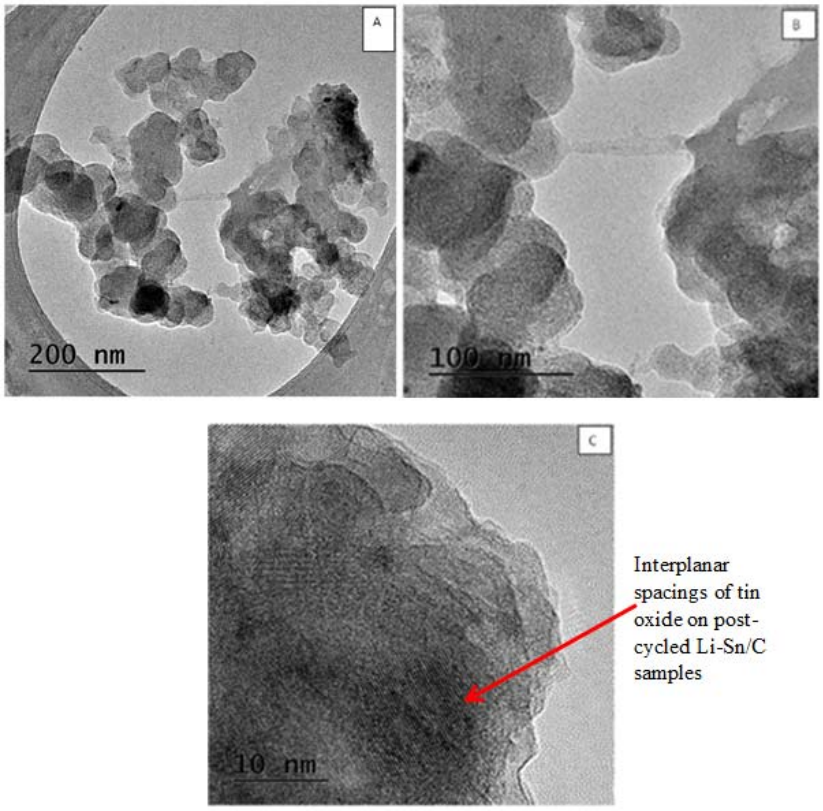

TEM characterization of post-cycled Li-Sn/C (10% Sn) sample. A/B: Post-cycled Li-Sn/C sample showing Sn on the carbon support. C: Small Sn particles showing interplanar spacing, measured to be presence of tin oxides. This could be due to exposure of nano Sn particles to oxygen during handling, which resulted in the formation of tin oxides.

Figure 45. TEM Images of Sn/C Na-ion Battery (Post Cycling).

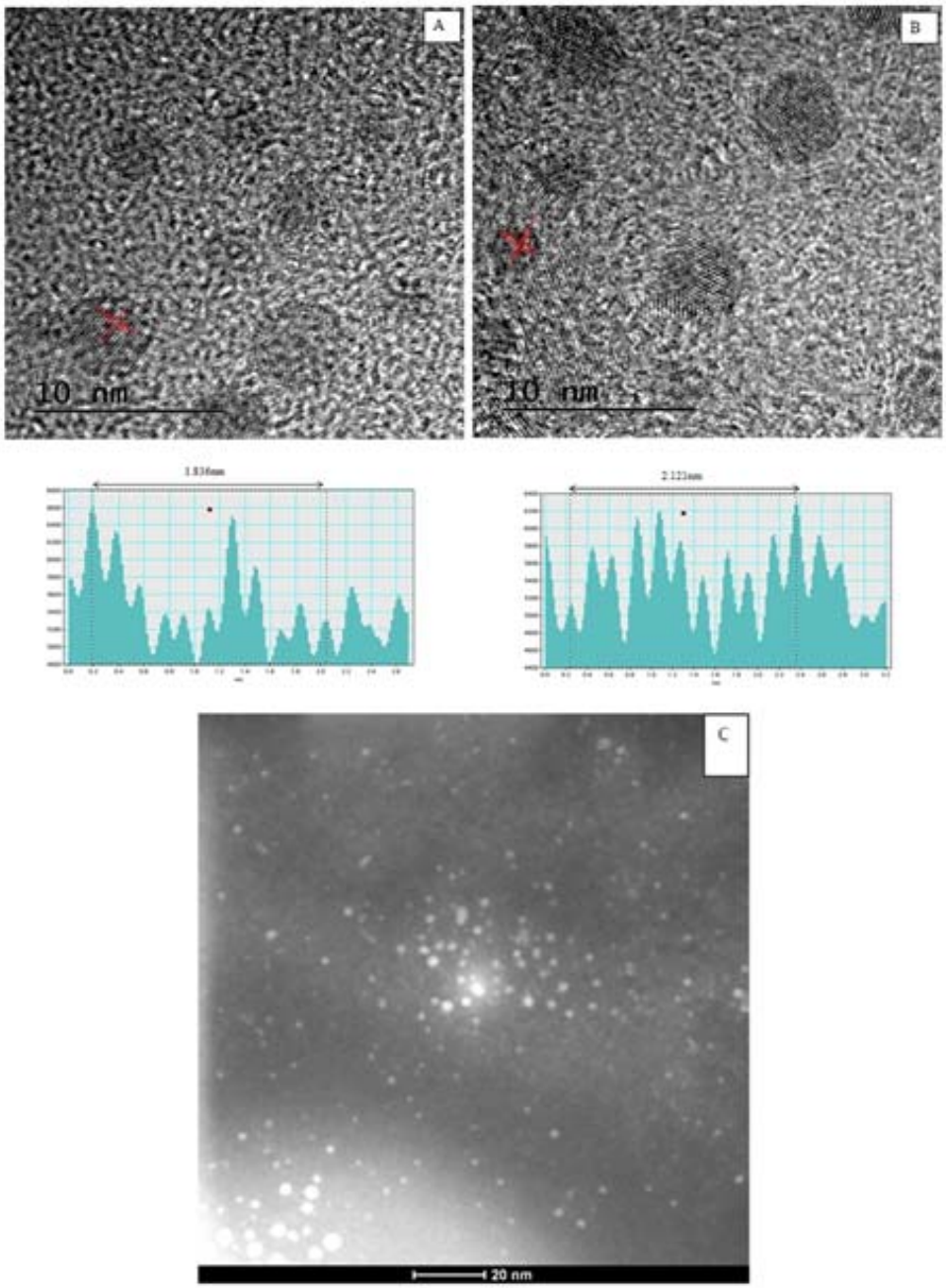

TEM characterization of post-cycled Sn/C Na-ion sample. A/B: Post-cycled Sn/C Na-ion sample showing Sn on the carbon support. Measurement of interplanar spacings showed presence of tin oxides. Again, it is postulated that tin oxides formed due to handling when pure nano-sized Sn was exposed to the air. Nonetheless, the presence of Sn signifies stability of linkages between Sn and C through the RES process, enabling it to withstand stresses due to cycling in a battery. C: Small tin oxide particles shown in a dark field image.

Figure 46. XRD Pattern Showing Presence of Sn after Cycling.

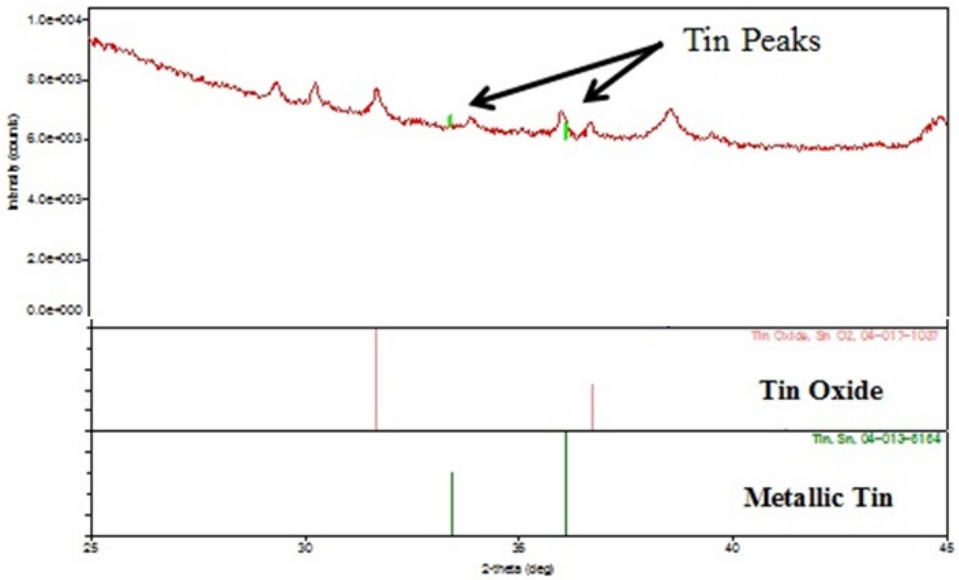

XRD pattern of post-cycled Sn/C in Li-ion battery. Presence of Sn found in Sn/C Li-ion battery cell after more than 100 cycles signifies remarkable stability of Sn/C linkages achieved by the RES process.

F. CHARACTERIZATION OF SN/C PRODUCED BY ATP

Having successfully created Sn/C samples using the RES technique, the study also looked at the feasibility of producing similar samples using the ATP technique. However, as discussed in the previous section, the sample produced from ATP was relatively small (0.01g) from each cycle. Inclusive of preparation time, the total time required to produce this 0.01g of sample was six hours. This would mean that a much longer time would be required to obtain the same amount of sample via RES. Hence, even though a successful sample was produced via ATP, it was deemed not to be commercially viable to produce larger amounts of sample for further studies. Thus, the Sn/C produced via ATP was not cycled in a battery cell. Nonetheless, the sample produced was characterized via XRD, SEM, EDS, and TEM (Figures 47–50).

Figure 47. XRD Pattern of ATP Produced Sample.

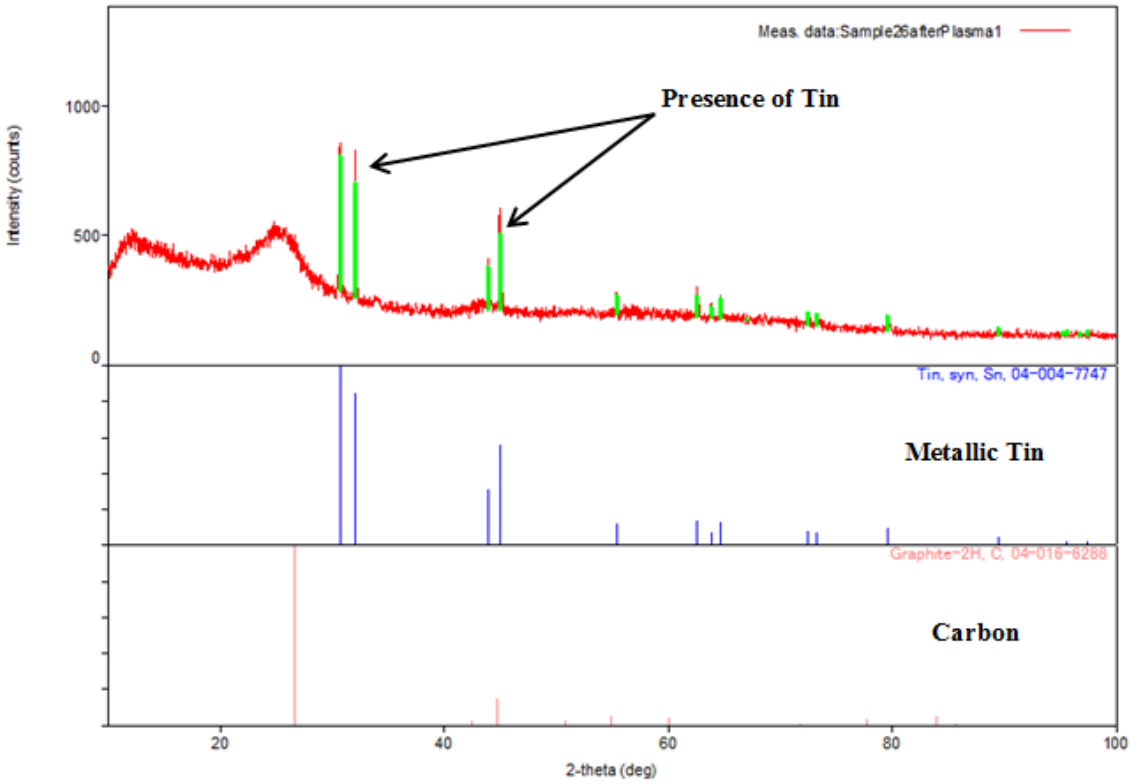

XRD pattern of ATP-produced Sn/C. Presence of pure Sn in Sn/C produced by ATP showed the ability of ATP to produce pure Sn particles on carbon support.

Figure 48. Tin Peak of ATP.

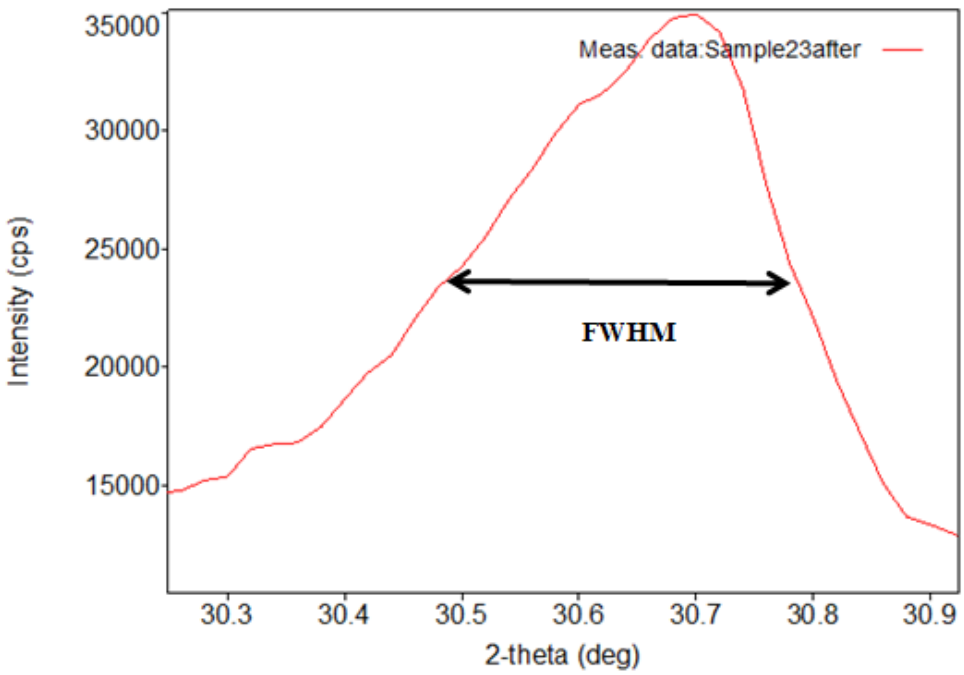

Enlarged XRD peak of Sn metal used to determine FWHM. Calculations via Debye Scherrer calculations show nano-sized (~30nm) particles in Sn/C produced by ATP.

Results from the XRD showed the presence of tin without the presence of tin oxide. In addition, the broad width of the tin peak indicates the presence of small particles of tin. This was validated with SEM of the ATP sample.

Figure 49. SEM Image of ATP Sample at 5000x Indicating Presence of Tin.

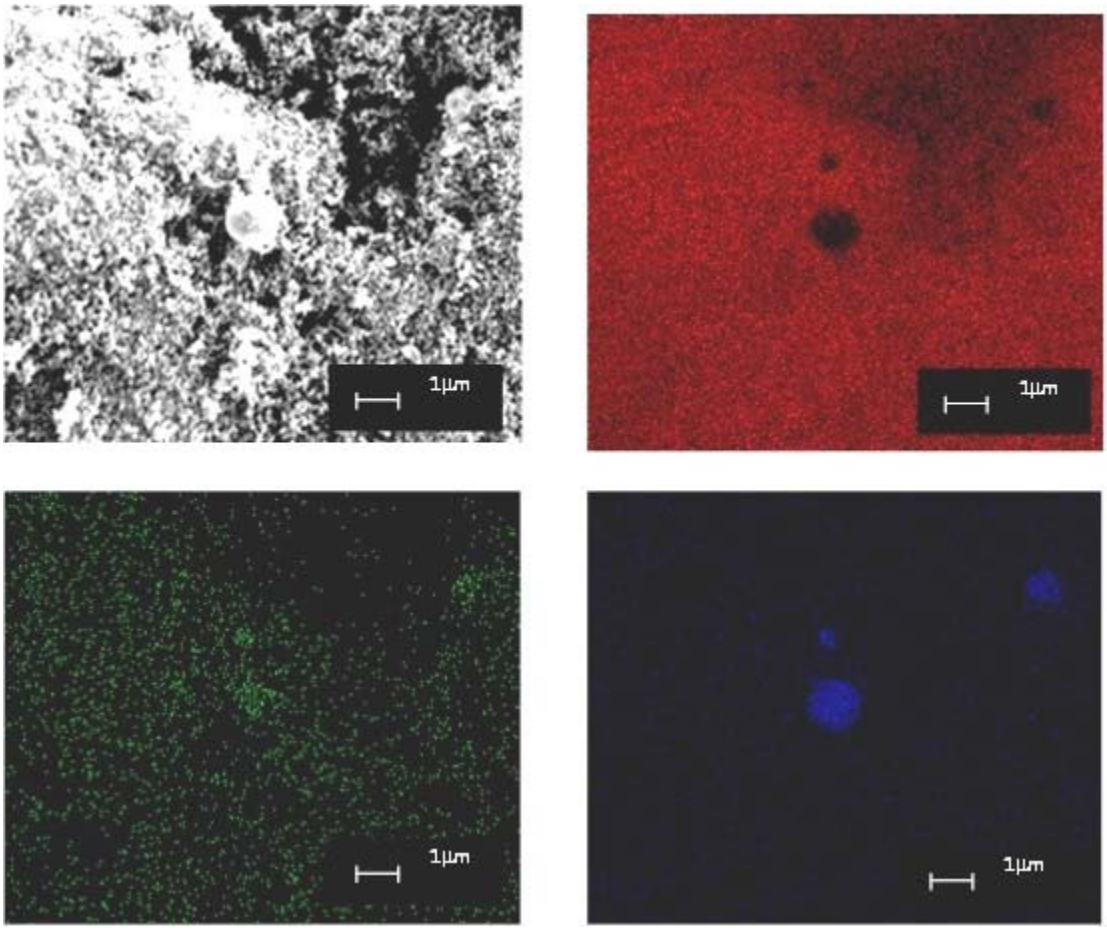

EDS Elemental Display of ATP-produced Sn/C. Top left (in clockwise direction): SEM image of Sn/C sample, Carbon Distribution (Red), Tin Distribution (Blue), Oxygen (Green).

Figure 50. TEM Image of ATP Sample at 360000X Showing Nano-Sized Particles.

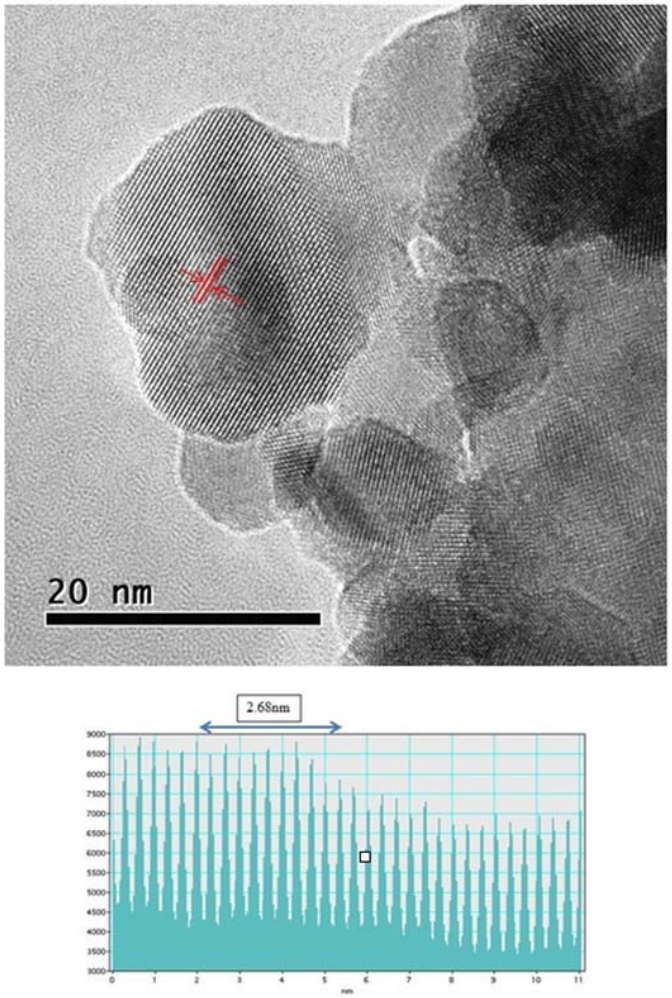

Measurement of interplanar spacings showed the presence of nano-sized Sn particles in Sn/C sample produced by ATP [42].

IV. DISCUSSION

This chapter summarizes the samples produced by RES and ATP with a short description on the overall success of this study.

A. SUMMARY OF RES SAMPLE

This study was designed to test the hypothesis that RES synthesis of Sn/C electrodes can lead to strong bonding between metal and support such that high levels of capacity by the electrodes can be maintained over hundreds of charge/discharge cycles. This hypothesis rested on several prior observations and a model of carbon surface chemistry.

The hypothesis was based both on theory and success of earlier experiments. The prime source of experimental support for the use of RES to produce small, stable Sn particles on carbon was an earlier success in which RES was used to produce unusually small and stable metal particles on a different support. That is, in an earlier study RES was employed to make unique platinum (Pt) rafts, approximately five atoms each on a conductive substrate for use in fuel cell electrodes. The formation of these rafts on the underlying conductive substrate was postulated to result from a sequence of chemical processes:

1. Generation of free radicals via thermal decomposition of urea,
2. Removal of surface oxygen atoms from the substrate by those reducing radicals consequently creating unsaturated surface sites,
3. Immediate bonding to these sites of Pt atoms released by thermal decomposition of a platinum atom containing precursor molecules.

The RES process clearly resulted in the creation of uniquely strong metal/ substrate bonds that prevented the type of Pt particle growth normally observed on fuel cell electrodes.

A number of other studies provide substantial support that RES synthesis can produce unique metal structures by reduction of precursor species via the thermal decomposition of urea. These reports do not involve the creation of particles on a

support; nevertheless, these reports do show the fundamental postulates of RES are consistent with observation. Specifically, RES was employed in the syntheses of graphene from mixtures of urea and graphite oxide, and the reduction of sub-micron scale metal particles from mixtures of urea and oxide, hydroxide, or nitrate precursors.

The qualitative theory of carbon surface chemistry also informed the experimental design. In order to explain more precisely the anticipated chemistry of RES generation of Sn/C electrodes, it is necessary to present a condensed description of a widely accepted model of the creation of unsaturated, "surface radical," sites on carbon. Generally, carbon, either graphitic or turbostratic, surfaces consist primarily of basal planes in which all atoms are strongly bonded to the three nearest neighbors. Little chemistry takes place here. In contrast, at defect sites, including edges, there are surface sites capable of chemistry. In particular, O atoms, OH complexes, etc., often bond to unsaturated carbon atoms at these sites. It is well documented that O groups, found at edges and defects, serve as the nucleation points for many processes including water adsorption and metal particle formation, but not strong bonding. However; there are specific methods to remove O species from these sites, such as heating to 950 degrees Celsius in flowing inert gas that remove C atoms as well, and concomitantly create dangling bonds or surface radicals. It is well documented that the surface radicals so formed can form strong bonds to metal atoms [43], [44].

Surface radicals concentration is a function of many factors, including gas phase identity and temperature. Thus, careful synthesis design is required. For instance, treating a carbon surface in hydrogen at temperatures above 950 degrees Celsius creates a hydrophobic, chemically inert carbon, not a surface with active radicals. High temperature treatment in hydrogen not only strips the oxygen groups from the surface, but also allows hydrogen gas to react with all surface radicals created by the removal of oxygen to create methane. No highly reactive surface sites remain. One of the simplest tests of this hypothesis is a test of hydrophobicity. A carbon surface without oxygen groups or surface radicals is hydrophobic. Hence, in studies conducted herein, untreated carbon was tested for hydrophobicity. In all cases, the untreated carbon was hydrophobic.

Returning to the hypothesis of this study, it is believed that during RES synthesis of the Sn/Cn electrodes, two steps, previously only carried out sequentially, are combined into a single rapid synthesis. Specifically, during the RES synthesis in an inert gas (N_2) conducted herein, reducing radicals produced via urea decomposition attack oxygen groups on the carbon surface, leading to the formation of volatile, stable species. This process leaves behind surface radicals on the carbon. Almost immediately, these surface radicals form strong bonds with metal atoms, also produced by radicals created by thermal decomposition of urea. These metal atoms are generated via the decomposition of metal precursor molecules, a process that is thermally driven and takes place concomitantly with the thermal decomposition of the urea.

All of the data collected in this study is consistent with the process outlined in the previous paragraph. In particular, these observations are consistent with the model, and each is discussed in more detail here:

1. Very small Sn particles formed (<20nm).
2. The small Sn particles are stable even at 800 C.
3. The Sn particles remain stable over hundreds of charge/discharge cycles for both Li and Na insertion.
4. The same RES synthesis carried out on O-atom free, hydrophobic carbon (control study) does not produce highly dispersed Sn particles, but rather micron scale, spherical Sn particles.

In turn, these results suggest directed efforts to create high capacity Sn/C electrodes using the RES method. For example, simply increasing the Sn loading during synthesis could substantially increase capacity with no sacrifice to stability. Also, different carbons used during RES synthesis may produce even greater stability. These will be briefly discussed in the final chapter on future recommendations.

Evidence for the various claims regarding particle size and stability in battery use is clearly found in the XRD, TEM, and SEM data provided in the results chapter. Indeed, the existence of very small Sn particles (<20 nm) after RES synthesis is found from SEM (Figures 34, 39) and TEM studies (Figures 35, 36, 44, 45). The XRD spectra of Sn/C clearly show very broad Sn metal lines, consistent with an average particle size per the

Debye Scherrer Equation, of 20 nm prior to the battery study (Figure 33). Evidence of the stability of Sn particles after 200 cycles of Li capacity testing was verified using the same XRD technique (Figure 46) and showed virtually no Sn particle growth. This is remarkable because in all prior studies in which Sn/C electrodes were synthesized and tested, there was dramatic Sn particle growth and/or Sn particle "crumbling" after less than 25 cycles of anode testing [45], [46].

Additional evidence of the existence and stability of very small metallic Sn particles during operation as an anode is also found from TEM studies. The particle sizes prior to anode testing, as shown in Figures 35 and 36, and those found after testing, shown in Figures 44 and 45, are very similar. There is no evidence of the kind of dramatic particle size growth usually found in conventionally synthesized Sn/C anodes [47].

There is indirect evidence of nanoscale particles of Sn before and after battery electrode study from SEM. Specifically, no particles of Sn are evident in the material generated using RES on hydrophilic Vulcan XC72 from SEM studies. This is a confirmation that the particles are very small. There is clearly substantial Sn in the sample, and the inability of the SEM to focus and display the image shows the particles to be very small. That is, 20 nm metal particles are at the limit of reliable detection using the available SEM. Consider the contrary case in which large particles were formed: RES on hydrophobic XC72. Indeed, virtually all the Sn was present as large (many micron) Sn particles on hydrophobic carbon. According to the model presented previously, this is expected because "surface radicals" will not form during RES synthesis on a hydrophobic carbon. In the absence of these radicals, bonding between and the carbon surface is very weak, leading to formation of weak carbon-oxygen-tin bonds. In turn, this leads to very rapid sintering of the Sn and the concomitant formation of micron-sized particles. In volumetric terms, the average particles seen to form on the hydrophobic support in SEM are about a million times larger than the average particle formed by RES on hydrophilic carbon. Hence, SEM was valuable in demonstrating a very different Sn particle growth process that occurs when not all the requirements for producing nano-scale Sn are present in the RES synthesis.

It is notable that the small particles observed using both TEM and XRD are from samples that contain 10% / 20% by weight of Sn. This is far higher metal loading than that employed in the related studies of RES synthesis of supported metal catalysts (<5%). Thus, this is the first indication that the process works to produce nano-scale particles at the high loadings required for practical battery electrode use.

A preliminary model for the capacity of Sn/C was also proposed (Figure 42) to extrapolate expected capacity with increased tin loading. However, given the limited number of data at this juncture, further testing and development is required to refine the proposed model.

B. SUMMARY OF ATP SAMPLE

The study has shown that the production of tin nanoparticles on a carbon support via ATP is possible. The precursors of micron-sized tin and carbon particles that pass through plasma under aerosol produce nano-sized tin particles scattered on the carbon support. This has been confirmed through characterization studies done by XRD (Figures 47, 48), SEM (Figure 49), and TEM (Figure 50) techniques. However, the process produces a very small amount of sample over a long period of time and is thus not a commercially viable option. Hence, further testing in a battery cell for Sn/C produced by ATP was not carried out in this study.

THIS PAGE INTENTIONALLY LEFT BLANK

V. CONCLUSION

The study has shown that the production of tin nanoparticles on a carbon support for the purpose of a sodium- or lithium-ion battery anode is successful via the RES method. In particular, there are two main benefits that can be derived from this study: benefits to the USN as well as to industry as a novel and proven method of battery fabrication.

A. BENEFITS TO THE USN

With the advancement of energy-dependent weaponry such as the rail gun and free electron laser, there is an increasing need to find a suitable energy storage medium for this new generation of arsenal. While the Zumwalt-class destroyer, the first all-electric ship in the USN, will provide a suitable platform to house these energy-dependent weapons, findings from this study will assist in this development from two aspects.

1. Potential Increase in Capacity from Lithium-ion Batteries

The result has proven that a higher capacity can be potentially derived from Li/Sn chemistry. This is because with $Li_{22}Sn_5$, the resulting high lithium packing density (75.47 mol L^{-1}) is comparable to that of pure lithium metal (76.36 mol L^{-1}), yielding a theoretical capacity of ~990 mAh/gSn. This is far better than that of the ultimate graphite electrode, ~370 mAh/gC. As shown from the study, an increase in tin loading of 10% Sn to 20% Sn yielded an increase of 18% capacity from 280mAh/g to 320 mAh/g. This shows immense potential in further increasing the capacity given that the choice of carbon as well as precursor ratio have yet to be optimized during the course of this study. Should such an Li-Sn/C battery be developed to achieve the stated capacities, it would assist greatly in the push of the new-generation of weaponry in the USN.

2. Reduced Reliance on Lithium-ion Batteries

The study has also proven that Na-ion batteries using Sn/C is also possible. Conventionally, batteries produced using Sn tend to last less than 25 cycles due to

volumetric increases (~300%) that result in crumbling of Sn within the battery. This study has proven that nano-scale Sn produced on a carbon support is not only able to withstand the stresses of volumetric expansion, it is also able to remain stable over long periods of charge and discharge cycles. Figure 44 shows the battery cell created using Sn/C in an Na-ion battery is able to remain stable over 500 cycles. Although the capacity shown in this study is relatively low (~100 mAh/g), subsequent studies to harness the remarkable stability may be a strategic asset in the future. With the limited lithium resource and increased competition for its usage, it may well be a strategic move for the USN to develop Na-ion batteries for the new generation of energy-dependent weapons.

B. NOVEL AND PROVEN METHOD OF BATTERY ANODE FABRICATION USING RES TECHNIQUE

More importantly, this study has proven that the RES technique is able to create remarkably small Sn particles on a carbon support, which remains stable over hundreds of cycle in a battery. In particular, the study has proven that the concept of creating a supported metal catalyst holds true in the fabrication of batteries, including:

- The activation of carbon is possible by heating the carbon support in air and removing the oxygen groups via the reduction phase of RES. This in turn produces dangling carbon bonds that are able to bond with the tin particles of the precursor.
- The tin bonds with the carbon support in a unique and strong manner. This has been proven by the cyclability of the Sn/C electrode under loading (up to 320 mAh/g, in excess of 100 cycles in lithium and in excess of 500 cycles in sodium), which shows that the volumetric increase of tin has been mitigated, avoiding the occurrence of sintering.
- The increase in Sn loading from 10% to 20% also showed an increase in capacity values for both Li- and Na-ion battery cycles. This means that Sn participated in the cycling process and shows promise for future development of higher capacity Sn/C electrodes.

It is noted that are still many areas of this study that can be improved and optimized to obtain potentially better capacity than seen in this study. The next chapter discusses the potential steps that can be taken to further refine the Sn/C anode.

VI. RECOMMENDATIONS FOR FUTURE WORK

A. ADJUSTING PROPORTION OF TIN IN PRECURSOR

The proportion of tin in the precursor can be further fine-tuned to maximize the amount of tin (and thus the energy density) in the Sn/C produced. Currently, the sample contains about 20% of tin in the tin/carbon sample. This could be potentially increased to >50% in order to improve the energy density of this anode. However, it is important to ensure that the final product continues to maintain nano-sized particles so as to avoid the occurrence of sintering. This is because the increase of the proportion of tin could also potentially create the agglomeration of tin particles during nucleation, thus producing larger sized tin particles.

B. CHANGING THE CARBON SUPPORT

Although this study shows the current carbon support (Vulcan XC72) to be a suitable carbon support to anchor the tin particles, further studies can be done to understand the type of carbon used. For instance, the research can be directed in determining whether the pore size and surface area of the carbon support affects the size of tin particles produced after the reduction process.

C. OPTIMIZATION OF PRECURSORS

The study has shown that the precursor of tin (II) chloride, urea, carbon, and water, mixed in the ratio of 1: 1: 2.5: 20 is able to produce a suitable Sn/C anode for battery cycling. However, further analysis can be made in optimizing the following aspects:

- Determining whether tin (II) chloride is a suitable salt in terms of solubility in water as part of the precursor.
- Determining whether the previously stated ratio can be optimized to reduce drying time.
- Determining the optimal Sn/Urea ratio to efficiently remove surface oxides during the RES process.

D. TESTING THE LIMITS OF CHARGE AND DISCHARGE CYCLES

In the course of this study, the focus was to demonstrate that the novel process of RES in creating Sn/C was successful. Hence, while cycling in Li-ion and Na-ion batteries, the limits of charge and discharge cycles were not determined. From the current data presented, it is shown that Sn/C anode remains stable over 100 cycles in Li and 500 cycles in Na. However, given the remarkable stability shown in the study as well as the small Sn particles that remained post-cycling, it is postulated that the Sn/C anode could possibly remain stable over longer periods of cycling. This could also be tested in future studies.

E. SCALING UP OF THE RES PROCESS

Currently, 1 gram samples are produced during each laboratory session. This could potentially be increased using a larger alumina boat and furnace. With larger samples, higher energy storage scenarios can be studied and analyzed. The larger furnace, boats, and quartz tubes have been purchased by the Naval Postgraduate School for this next stage of development. However, for larger samples, there must be an emphasis on the distribution of the tin particles throughout the precursor. As determined by one of the experiments, if the distribution is not done in a homogeneous manner, samples produced on the top and bottom layer could be different.

F. DEVELOPING IN-HOUSE MEASUREMENT CAPABILITY

As the current battery tests were done by a partner university, this researcher had to verify the data to ensure credibility of the information received. As it is, there are certain areas of the battery testing results that still require further understanding and analysis. In addition, it takes at least three to six weeks for the latest sample to be sent and for the results to be retrieved. To avoid such ambiguity and expedite the measurement of the battery, it is recommended the Naval Postgraduate School develops in-house measurement capability. This will allow students to have faster access to the results of their sample. Given the increasing role of the Materials Department in developing new battery materials for the USN, in-house measuring capability will also put the department in good stead for future testing and development.

APPENDIX

The following table shows the full suite of experiments conducted during the course of this study. Objectives of and remarks about the various experiments are stated herein.

Experiment	Objective	Precursor Used	Remarks
1 (24 Nov 15)	Fabrication of Sn/C sample with *inactivated* carbon support	Tin Acetate: 0.504g Urea: 1.917g Carbon: 2.539g Water: 1.938g	• Precursor was hand ground and flushed with nitrogen at 100 sccm for 10 minutes • Heated at 800 degrees Celsius at 5 sccm for 3.5 minutes during RES process • XRD revealed only tin oxides in sample • No presence of Sn • Carbon was not activated and was thus hydrophobic • Wetting of carbon revealed formation of spherical particles on the surface of the carbon • Tin acetate was used in this series of experiments
2 (4 Dec 15)		Tin Acetate: 1.029g Urea: 0.9945g Carbon: 2.505g Water: 2.192g	
3 (8 Dec 15)		Tin Acetate: 1.029g Urea: 0.9945g Carbon: 2.505g Water: 2.192g	
4 (7 Jan 16)	To determine parameters of carbon activation	Refer to Table 1	• Weight loss of 11% was found to be optimum for activation • Carbon became hydrophilic and wetting revealed water to be readily absorbed onto the carbon surface
5 (14 Jan 16)			
6* (21 Jan 16)	Fabrication of Sn/C using activated carbon and tin chloride in precursor (refinement of experiment 3)	Tin(II) Chloride: 0.349g Urea: 0.34g Carbon: 0.8683g Water: 6.9456g	• First successful detection of pure Sn in Sn/C sample • Sn particles were found to be in the order of 20 to 30 nm • Use of tin(II) chloride due

Experiment	Objective	Precursor Used	Remarks
			to better solubility in water compared to tin acetate • Activated carbon allowed more water to be absorbed and thus better distribution of tin particles on the carbon support
7 (19 Feb 16)	• Determine if sample 6 results are repeatable • Determine shortest time to achieve repeatable results	Tin(II) Chloride: 0.3979g Urea: 0.3956g Carbon: 0.7935g Water: 7.8856g	• Sample heated to 700 degrees Celsius (instead of 800) for 90 seconds (instead of 5 mins) • Only tin oxides were detected • Insufficient time and temperature for reduction to take place
8* (25 Feb 16)	To improve distribution of tin through ultrasound mixing (refinement of experiment 6)	Tin(II) Chloride: 0.399g Urea: 0.4046g Carbon: 0.986g Water: 7.996g	• Sample underwent drying process for 2 hours (instead of 1 hour) at 100 degrees Celsius • Sample was heated to 810 degrees Celsius for 5 minutes • Higher proportion of Sn was detected compared to sample 6
9 (10 Mar 16)	Control for inactivated carbon	Tin(II) Chloride: 0.4076g Urea: 0.4033g Carbon: 1.011g Water: 8.042g	• Carbon heated in nitrogen only at 610 degrees Celsius • Heated to 830 degrees Celsius for 5 minutes during RES process • Pure Sn was produced. However, particle size was large (microns).
10 (30 Mar 16)		Tin(II) Chloride: 0.401g Urea: 0.4045g Carbon: 0.9716g Water: 8.016g	
11* (6 Apr 16)	Increase of urea/Sn ratio as a means to better remove surface oxides	Tin(II) Chloride: 0.415g Urea: 0.609g Carbon: 1.03g	• Mixture was hand grinded for 10 minutes and placed in an ultrasound for 20 minutes

Experiment	Objective	Precursor Used	Remarks
	(refinement of experiment 8)	Water: 8.06g	• Mixture underwent drying process for 2 hours at 100 degrees Celsius • Heated to 810 degrees Celsius for 5 minutes during RES process • High intensity of Sn compared to tin oxide • Increasing urea/Sn ratio improves removal of surface oxides • Large Sn particle size (microns)
12* (13 Apr 16)	Reduce presence of oxygen by introducing dissolved tin chloride and urea to carbon support using a pipette (refinement of experiment 8)	Tin(II) Chloride: 0.4039g Urea: 0.401g Carbon: 1.0142g Water: 8.027g	• Only Sn particles were detected • However, there was not means of mixing while doing this experiment in an inert atmosphere • Top layer of sample observed to have much higher intensity of tin compared to lower layer • Particle size remained large (microns)
13 (20 Apr 16)	Recreation of experiment 8	Tin(II) Chloride: 0.397g Urea: 0.3963g Carbon: 1.006g Water: 7.982g	• Similar results to experiment 8
14 (27 Apr 16)	Reduce urea/Sn ratio and observe proportion of Sn (control for experiment 11)	Tin(II) Chloride: 0.4005g Urea: 0.197g Carbon: 0.9285g Water: 8.01g	• Proportion of tin oxide is higher due to less reducing agent present
15 - 20 (29 Apr to 19 May 17)			• Results had unexpectedly higher proportion of tin oxides • Leak detected in quartz

Experiment	Objective	Precursor Used	Remarks
			tube resulting in increased proportion of tin oxides
21 (23 May 16)	To determine whether a shorter burning time results in shorter growth period, resulting in smaller Sn particles	Tin(II) Chloride: 0.400 Urea: 0.400g Carbon: 1.039g Water: 8.001g	• Precursor was only hand ground as it is theorized that due to the carbon used, mechanical grinding can better distribute Sn particles • Heated at 800 degrees Celsius but only held for 30 seconds • Higher proportion of Sn compared to tin oxide.
22 (25 May 16)	Variation of experiment 9 but without ultrasound mixing	Tin(II) Chloride: 0.395 Urea: 0.399g Carbon: 0.984g Water: 7.999g	• Same results as experiment 9
23* (25 May 16)	Change of carbon support to Cabot Vulcan XC72	Tin(II) Chloride: 0.399 Urea: 0.399g Carbon: 0.994g Water: 8.001g	• Vulcan XC72 carbon is a finer carbon compared to the previous version. This provides a better means of distribution for the tin particles. With more nucleation sites, smaller Sn particles can be formed. • Successfully created Sn/C sample with high proportion of Sn and negligible amount of tin oxides • Sn particles found to be remarkably small in the order of 2nm
			• Sample has been placed in a battery and undergone 250 cycles in a Li-ion cell and 500 cycles in a Na-ion cell • Post-cycling analysis revealed that Sn particles were present and remained very small (<20 nm according to Debye Scherrer calculation)

Experiment	Objective	Precursor Used	Remarks
			• RES produced Sn/C able to withstand volumetric expansion and achieve stability after 500 cycles
24 (1 Jun 16)	Control to confirm first amorphous peak belonged to carbon support	Tin(II) Chloride: Not used Urea: 0.399g Carbon: 0.999g Water: 7.99g	• Amorphous peak confirmed to belong to Vulcan XC72 carbon support
25 (8 Jun 16)	Repeat of experiment 23	Tin(II) Chloride: 0.4007g Urea: 0.4007g Carbon: 0.998g Water: 8g	• Similar results to experiment 23
26* (15 Jul 16)	Sn/C produced via ATP	Pure Sn (micro): 0.2616g Carbon: 1.0048g	• Nano-sized Sn particles produced • However, production took a much longer time to produce only 0.0095g of Sn/C
27/28 (22 Jul 16)	Production of experiment 23	Tin(II) Chloride: 0.4045g Urea: 0.4030g Carbon: 1.0057g Water: 8.0125g	Similar results to experiment 23
29* (Nov 17)	Double tin loading to 20%	Tin(II) Chloride: 1.074g Urea: 1.073g Carbon: 1.004g Water: 8.02g	• Higher proportion of Sn compared to experiment 23 in the precursor • Higher capacity compared to experiment 23 after cycling • Cycled in excess of 250 cycles

* Significant milestones during the study

THIS PAGE INTENTIONALLY LEFT BLANK

LIST OF REFERENCES

[1] B. Wright. (2016, Jun. 27). Is U.S. Navy railgun electromagnetic cannon cost too expensive? Despite drawbacks, officials tout new weapon *International Business Times.* [Online]. Available: http://www.ibtimes.com/us-navy-railgun-electromagneticcannon-cost-too-expensive-despite-drawbacks-officials-2387188

[2] US Navy plans for scaling free electron lasers to megawatt weapon systems. (2016, Mar. 4). The Next Big Thing. [Online]. Available: http://www.nextbigfuture.com/2016/03/us-navy-plans-for-scaling-free-electron.html

[3] Zumwalt class destroyer. Raytheon. [Online]. Available: http://www.raytheon.com/capabilities/products/zumwalt/. Accessed Jan. 14, 2017.

[4] S. Jewell and S. M. Kimball, "Mineral commodities summary 2016," *U.S. Geolog. Survey*, Reston, VA, Jan. 2016.

[5] A. D. Jialiang Tang, "Advancement in sodium-ion rechargeable batteries," *Sci. Direct Current Opinion Chem. Eng.*, vol. 9, pp. 34–41, Aug. 2015.

[6] E. Venere. (2015, Sep. 22). Sodium-ion batteries are potential power technology of future. [Online]. Available: http://www.purdue.edu/newsroom/releases/2015/Q3/sodium-ion-batteries-are-potential-power-technology-of-future.html

[7] M. Winter and J. O. Besenhard, "Electrochemical lithiation of tin and tin-based intermetallics and composites," *Electrochimica Acta*, vol. 45, pp. 31–50, 1999.

[8] A. Courtney and J. R. Dahn, "Electrochemical and in situ x-ray diffraction studies of the reaction of lithium with tin oxide composites," *J. Electrochem. Soc.*, vol. 144, pp. 2045–2057, 1997.

[9] S. Goriparti, E. Miele, F. De Angelis, E.Di Fabrizio, R. P. Zaccaria, and C. Capiglia, "Review on recent progress of nanostructured anode materials for Li-ion batteries," *J. Power Sources*, vol. 257, pp. 421–443, 2014.

[10] T. Watkins. (2016, Jun. 25). U.S. Navy keeps electromagnetic cannon in its sights. [Online]. Available: http://phys.org/news/2016-06-navy-electromagnetic-cannon-sights.html

[11] R. Smith. U.S. Navy's Mach 7 railgun could mean billions of dollars for General Dynamics. The Motley Fool [Online]. Available: http://www.fool.com/investing/general/2016/02/21/us-navys-mach-7-railgun-billionsgeneral-dynamic.aspx. Accessed Aug. 16, 2016.

[12] C. P. Cavas. (2016, Jan. 10). Navy's rail gun still headed to sea, but on which ship? [Online]. Available: http://www.defensenews.com/story/defense/naval/ships/2016/01/10/railgun-navy-fanta-naval-zumwalt-ddg1000/78443016/

[13] S. Chappell. Free electron laser. [Online]. Available: http://www.onr.navy.mil/Media-Center/Fact-Sheets/Free-Electron-Laser.aspx. Accessed Aug. 16, 2016.

[14] B. Lendon. (2014, Apr. 10). Navy's future: Electric guns, lasers, water as fuel. *CNN* [Online]. Available: http://www.cnn.com/2014/04/10/tech/innovation/navy-new-technology/

[15] T. Casey. (2013, Nov. 5). Navy's new "all-electric" destroyer is a seagoing microgrid. [Online]. Available: https://cleantechnica.com/2013/11/05/us-navy-launches-new-all-electric-zumwalt-destroyer/

[16] R. Ellis. Electromagnetic railgun. [Online]. Available: http://www.onr.navy.mil/~/media/Files/Fact-Sheets/35/Electromagnetic%20Railgun_Dec%2029%202014.ashx. Accessed Aug. 18, 2016.

[17] Captain David H. Kiel, C. M., "A vision for directed energy and electric weapons," unpublished.

[18] Y. N. Liu, "Ultrasmall Sn nanoparticles embedded in carbon as high- performance anode for sodium-ion batteries," *Adv. Funct. Mater.*, vol. 25, issue 2, pp. 214–220, Jan. 2014.

[19] J. Wang et al. "Structural evolution and pulverization of tin nanoparticles during lithiation-delithiation cycling," *J. Electrochem. Soc.*, vol. 161, no. 11, pp. 3019–3024, Jun. 2014.

[20] P. L. Walker, *Chemistry and Physics of Carbon: A Series of Advances.* New York: Dekker, 1965.

[21] S. Wakeland, Y. Cui, A. Knapp, M. Richard, J. Phillips, and C. Luhrs. "Multilayered nanoparticles generated by plasma methods for energy storage applications," *Nanosci. and Nanotechnol. Letters*, vol. 4, pp. 316–322, Mar. 2013.

[22] W. M. Zhang, J. S. Hu, Y. G. Guo, S. F. Zheng, L. S. Zhong, W. G. Song, and L. J. Wan, "Tin-nanoparticles encapsulated in elastic hollow carbon spheres for high-performance anode material in lithium-ion batteries," *Adv. Mater*., vol. 20, pp. 1160–1165, Mar. 2008.

[23] K. T. Lee, Y. S. Jung, and S. M. Oh, "Synthesis of tin-encapsulated spherical hollow carbon for anode material in lithium secondary batteries," *J. Am. Chem. Soc*., vol. 125, pp. 5652–5653, Apr. 2003.

[24] G.-L. Cui, Y.-S. Hu, L.-J. Zhi, D.-Q. Wu, I. Frieberwirth, and J. Maien, “A one-step approach towards carbon-encapsulated hollow tin nanoparticles and their application in lithium batteries,” *Small*, vol. 3, pp. 2066–2069, Nov. 2007.

[25] P. L. Walker Jr., M.D., *Chemistry and Physics of Carbon,Volume 2*. Pennsylvania: Pergamon Press, Ltd., 1966.

[26] J. A. Menendez, J. Phillips, B. Xia, L. R. Radovic, “On the modification and characterization of chemical surface properties of activated carbon: In the search of carbons with stable basic properties,” *Langmuir*, vol. 12, no. 18, pp. 4404–4410, Sep. 1996.

[27] J. Phillips and B. Xia, “Calorimetric study of oxygen adsorption on activated carbon,” *Thermochimica Acta*, vol. 312, issues 1–2, pp. 87–93, Mar. 1998.

[28] J. Phillips, D. Kelly, L. R. Radovic, B. Xia, “Microcalorimetric study of the influence of surface chemistry on the adsorption of water by high surface area carbons,” *J. Phys. Chem.*, vol. 104, issue 34, pp. 8170–8176, Aug. 2000.

[29] K. Skokova and L. Radovic, “On the role of carbon-oxygen surface complexes in thecarbon/oxygen reaction mechanism,” *American Chemical Society, Division of Fuel Chemistry*, vol. 41, issue 1, Dec. 1996.

[30] A. A. Chen, M. A. Vannice, J. Phillips, “Effect of support pretreatments on carbon-supported Fe particles,” *J. Phys. Chem.*, vol. 91, issue 24, pp. 6257–6269, Nov. 1987.

[31] J. A. Menendez, B. X.,” On the Modification and Characterization of Chemical Surface Properties of Activated Carbon: Microcalorimetric, Electrochemical, and Thermal Desorption Probes,” *Langmuir*, vol. 13, no. 13, pp. 3414–3421, 1997.

[32] C. C. Luhrs, J. Phillips, “Reductive-expansion synthesis of graphene,” U.S. Patent 8 894 886, Mar. 4, 2011.

[33] L. Elbaz, J. Phillips, K. Artyushkova, K. More, E. Brosha, “Evidence of high electrocatalytic activity of molybdenum carbide supported platinum nanorafts,” *J. Electrochem. Soc.*, vol. 162, no. 9, pp.681–685, 2015.

[34] H. Soliman, J. Phillips, C. C. Luhrs, H. Zea, and Z. C. Leseman, “Aerosol synthesis of nano and microscale zero valent nickel particles from oxide precursors,” in *Proceedings ASME Micro-ElectroMechanical Systems (MEMS) 2010*, IMECE2010-39075, 2010.

[35] C. C. Luhrs, M. Kane, Z. Leseman, and J. Phillips, “Novel process for solid state reduction of metal oxides and hydroxides,” *Metal. and Mater. Trans B*, vol. 44, pp. 115–122, Feb. 2013.

[36] C. C. Luhrs, Z. Leseman, J. Phillips, H. R. Zea, “Generation of metal and alloy micron, submicron or nano particles in simple, rapid process,” U.S. Patent 8 709 126, Apr. 29, 2014.

[37] J. Phillips, “Plasma generation of supported metal catalysts,” U.S. Patent 5 989 648, Nov. 23,1999.

[38] J. Phillips, C. C. Luhrs, M. Richard, “Review: Engineering particles using the Aerosol-Through-Plasma Method,” *IEEE Transactions on Plasma Science*, pp. 726–739, 2009.

[39] H. Zea, J. Phillips, et al., “Plasma torch generation of carbon supported metal catalysts,” *Catalysis Today*, vol. 89, no. 1–2, pp. 237–244, 2004.

[40] A. I. Osman. (2016, Jul. 24). How do I calculate nanocrystallite size by Debye Scherrer equation using XRD. [Online]. Available: https://www.researchgate.net/post/How_do_I_calculate_nanocrystallite_size_by_Debye-Scherrer_equation_using_XRD. Accessed Jun. 21, 2016.

[41] Y. Xu, Y. Zhu, Y, Liu, C. Wang, “Electrochemical performance of porous carbon/tin composite anodes for sodium-ion and lithium-ion batteries,” *Adv. Energy Mater*., vol. 3, issue 1, pp. 128–133, Jan. 2013.

[42] International Centre for Diffraction Data. SnO2 00–021-1250. Accessed Jan. 30, 2017.

[43] J. Phillips, B. Clausen, and J. A. Dumesic. “Iron pentacarbonyl decomposition over grafoil I: Production of small metallic iron particles,” *J. Phys. Chem.*, vol. 84, issue 14, pp. 1814–1822, Jul. 1980.

[44] E. Hegenberger, N. L. Wu, and J. Phillips, “Evidence of strong interaction between iron particles and an activated carbon support,” *J. Phys. Chem*., vol. 91, issue 19, pp. 5067–5071, Sep. 1987.

[45] S. Yang, P. Y. Zavalij, M. S. Whittingham, “Anodes for lithium batteries: Tin revisited,” *Electrochem. Commun.*, vol. 5, no. 7, pp. 587–590, Jul. 2003.

[46] J. Hassoun, S. Panero, P. Reale, and B. Scrosati, “A new type of lithium-ion battery based on tin electroplated negative electrodes,” *Int. J. Electrochem. Sci*., vol. 1, no. 3, pp. 110–121, Jul. 2006.

[47] L. Q. Zhang, X. H. Liu, Y. C. Perng, K. Cho, J. P. Chang, S. X. Mao, Z. Z. Ye, and J. Y. Huang, “Direct observation of Sn crystal growth during the lithiation and delithiation processes of SnO2 nanowires,” *Micron*, vol. 43, no. 11, pp. 1127–1133, Nov. 2012.

INITIAL DISTRIBUTION LIST

1. Defense Technical Information Center
   Ft. Belvoir, Virginia

2. Dudley Knox Library
   Naval Postgraduate School
   Monterey, California